ARTICLE
Infectious Diseases Research 2024;5(1):3. https://doi.org/10.53388/IDR2024003

Antiplasmodial mechanism of *Lawsonia inermis*: An in silico based investigation

Ridwan Abiodun Salaam[1], Funmilayo I. D. Afolayan[1*]

[1]Department of Zoology, University of Ibadan, Ibadan 200005, Nigeria.

[*]**Correspondence to:** Funmilayo I. D. Afolayan, Department of Zoology, University of Ibadan, Ibadan 200005, Nigeria. E-mail: fidifede@gmail.com.

Author contributions

Conception and design: Afolayan Funmilayo and Salaam Ridwan. Experiment and analysis: Afolayan Funmilayo and Salaam Ridwan. Original manuscript drafting and revision: Afolayan Funmilayo and Salaam Ridwan. Final Approval: All authors.

Competing interests

The authors declare no conflicts of interest.

Peer review information

Infectious Diseases Research thanks drsunil, Hai-jun Gao and another anonymous reviewer for their contribution to the peer review of this paper.

Abbreviations

WHO, World Health Organization; CDC, Centres for Disease Control and Prevention; *P. falciparum*, *Plasmodium falciparum*; LIL, *Lawsonia inermis* Leaves; *L. inermis, Lawsonia inermis*; ADMET, Absorption, Distribution, Metabolism, Excretion, and Toxicity; OMIM, Online Mendelian Inheritance in Man; NCBI, National Centre for Biotechnology Information; NIST, National Institute of Standard and Technology; SEA, Similarity Ensemble Approach; PPI, Protein-Protein Interaction; KEGG, Kyoto Encyclopaedia of Genes and Genomes; BP, Biological Processes; MF, Molecular Functions; CC, Cellular Components; MCC, Maximal Clique Centrality; GSK3β, Glycogen synthase kinase-3 beta; MAPK1, Mitogen Activated Protein Kinase 1; IDO1, Indoleamine-2,3-dioxygenase 1; SPHK1, Sphingosine kinase 1; SDF, Structure Data File; SRC, Proto-oncogene tyrosine-protein kinase; PDGFRβ, Platelet-derived growth factor receptor β; RMSF, Root Mean Square Fluctuation; Rg, Radius of gyration; RMSD, Root Mean Square Deviation; VEGFA, Vascular endothelial growth factor A; HSP90AA1, Heat shock protein 90-alpha; PfHSP90, Plasmodium falciparum Heat Shock protein 90-alpha; TNF-alpha, Tumour Necrosis Factor; NOS2, Nitric Oxide Synthase 2; IL, Interleukin; IFN-gamma, Interferon-gamma; TGF, Transforming Growth Factor; MMP9, Matrix metalloproteinase 9; HMOX1, Heme Oxygenase 1; TLR4, Toll-Like Receptor 4; VCAM1, Vascular cell adhesion molecule 1; PRKACA, Protein Kinase CAMP-Activated Catalytic Subunit Alpha; CDK5, Cyclin-dependent kinase-5.

Citation

Afolayan FID, Salaam RA. Antiplasmodial mechanism of *Lawsonia inermis*: An in silico based investigation. *Infect Dis Res*. 2024;5(1):3. doi: 10.53388/IDR2024003.

Executive editor: Man-jin Tian.

Received: 26 December 2023; **Accepted:** 6 February 2024; **Available online:** 6 February 2024.

Abstract

Background: *Lawsonia inermis* has been widely reported to be used as an herbal treatment for Malaria. However, despite several experimental studies about its antimalarial activities, the approach through which the herbal plant suppresses plasmodium infection is yet to be found. Consequently, this study uses computational approaches to understand the biological targets and pathways involved in the antiplasmodial activities of *Lawsonia inermis* compounds. **Methods:** The Gas Chromatography-Mass Spectrometry technique identified the phytocompounds present in the herbal plant. GeneCards, OMIM, and NCBI databases were explored to collate target proteins for further network pharmacology analysis. The phytocompounds were subjected to Absorption, Distribution, Metabolism, Excretion and Toxicity (ADMET) and druglikeness analysis. The STRING algorithm and Cytoscape were employed to develop and analyze the relationships among target proteins and compounds/targets/pathways network of the putative targets of the phytocompounds. Further computational analysis was carried out to identify potential drug leads. **Results:** Based on the Network Pharmacology studies, phytocompounds in *Lawsonia inermis* exhibit antiplasmodial activity by interacting with therapeutic genes that play essential roles in metabolism and signaling pathways. Notable among the genes are MMP9, MAPK1, HMOX1 and IDO1. Meanwhile, the most influenced pathways include the metabolic pathway, PI3K-Akt signaling pathway, and HIF-1 signaling pathway. ADMET analysis, molecular docking analysis, and molecular dynamics simulation revealed that 3-phenyl-2-Isoxazoline and 2-Dimethylamino-3'-methoxyacetophenone are recommendable drug leads for Malaria treatment as they form stable and favorable complexes with Matrix metalloproteinase-9 (MMP9) target. **Conclusion:** The 3-phenyl-2-Isoxazoline and 2-Dimethylamino-3'-methoxyacetophenone phytocompounds from *Lawsonia inermis* herbal plant are predicted as antimalarial drug candidates and recommended for further wet-lab studies.

Keywords: *Lawsonia inermis*; computational studies; *plasmodium falciparum*; network pharmacology; molecular dynamic

Introduction

Malaria results from infection by plasmodium species parasites. These protozoans are transmitted by the female Anopheles mosquitoes. Plasmodium falciparum is responsible for the majority of Malaria cases in Africa [1]. Globally, vector control with long-lasting insecticide-treated bed nets, early diagnosis and treatment with combined drugs are the most used approaches to limit the incidence of Malaria. Also, chemoprevention is another widely used strategy, especially in pregnant women and young children [2]. Nevertheless, Malaria remains a major threat to human lives, especially in African countries, including Nigeria [3]. In 2022, about 94 % and 95 % of global Malaria cases and deaths, respectively, occurred in Africa, with children below the age of five years covering close to 78 % of total Malaria-related details in the continent. Out of this proportion, Nigeria suffers the highest percentage of Malaria deaths, with 26.8%, while the Democratic Republic of the Congo, Uganda, and Mozambique covered 12.3 %, 5.1 %, and 4.2 %, respectively [4]. Hence, it is apparent that Malaria is a major source of death and health concern in Nigeria, Africa, and beyond.

Plasmodium falciparum infection is largely accountable for the development of Malaria signs and symptoms. Depending on the severity of the condition, it could be acute or chronic, especially when treatment is lacking. In any population, young children without partial immunity against Malaria, pregnant women, especially during the first and second pregnancies, and travelers are the most susceptible groups to Malaria. Thus, Malaria has a massive social and economic toll on the people, ranging from the cost of drug purchase, loss of working days, poor health, expenses of preventive measures, cost of control and public health intervention, etc. [5].

However, Malaria is not only preventable but treatable. The treatment depends largely on the Plasmodium species that cause the infection burden, the severity, the patient's age, the cost of medicine, the availability of the drug, and the susceptibility of infecting species to antimalarial treatments [6]. According to Mishra et al., most available antimalarial drugs focus on the erythrocytic stage (asexual phase) of the infection, which leads to complications and symptoms [7]. On the contrary, the hepatic stage (pre-erythrocytic stage) is less attractive as an area of target due to fewer clinical manifestations. For instance, antifolates, such as pyrimethamine and cycloguanil, inhibit dihydrofolate reductase (DHFR), while notable drug-targeting proteins, including Ribosyldihydronicotinamide dehydrogenase in the hepatic stage, include Primaquine. The popular artemisinin is known to alkylate proteins and lipids [8]. Malaria treatment seeks to eliminate the parasite rapidly from the blood of the patient to limit the progression of non-severe Malaria to severe Malaria that could lead to death [6].

Malaria infections are treated using five groups of chemical compounds. They include artemisinin, quinolines, antifolates, antibacterial agents, and hydroxynaphthoquinones, as well as their derivatives [9]. However, these antimalaria drugs have been increasingly reported to face resistance by Plasmodium pathogens, making their eradication difficult and treatment challenging [9]. For instance, mutations in DHFR in cytosol have made the pathogen resistant to antifolate-based treatment. Also, a single point mutation in the cytochrome b subunit of the bc1 complex helped the pathogen to stand a chance against naphthoquinones, while mutations in K13 protein assist *Plasmodium falciparum* in the fight against Artemisinin-based treatment [9]. Thus, the need to discover and develop new potent drug molecules that can interact with multiple targets to stay ahead of the resistance curve of these pathogens is crucial. Fortunately, the World, especially Nigeria in Africa, is blessed with several plants with pharmacological relevance. In fact, several modern drugs, including artemisinin, have been made from local plants and traditional knowledge about medicine [10]. Based on ethnobotanical studies, many plants have been reported to have antimalarial properties with roots, leaves, fruits, stems, rhizomes, gum, and bark, commonly used to make a concoction for Malaria treatment [11, 12].

Among the commonly reported plants with antimalarial properties is *Lawsonia inermis*, commonly known as Henna in Nigeria. The *Lawsonia inermis* (Leaves) is widely used as a cosmetic dye for commercial purposes in Nigeria, northern African countries, and across Asia. More importantly, it has been reported to be used in treating skin problems, jaundice, amebiasis, diarrhea, leprosy, fever, leucorrhoea, diabetes, cardiac disease, and Malaria [13, 14]. Some wet-lab studies have been carried out to assess the antiplasmodial activities of the leaf extract of Henna. In 2016, an *in vitro* combination of *Lawsonia inermis* and *T. diversifolia* extracts was reported to show high synergy against *P. falciparum*, while a synergy with more than 80 % chemo-suppression was reported against P. berghei-infected mice [14]. In a different study, the antiplasmodial activity of *Lawsonia inermis* against Cameroon strains of *P. falciparum* has been reported [15]. Also, the ethyl-acetate of the henna leaves extract and fraxetin were found to be effective in an *in vivo* assay against *P. Berger*. Additional results from the study showed a twice as significant increase in mean survival time, an increase in catalase, superoxide dismutase and glutathione and a notable reduction in lipid peroxidation, which is also supported by the outcome of the study conducted by [16]. A post-infection treatment also enhances the endogenous antioxidant enzymes in comparison to the infected control mice. A more recent comprehensive review on the therapeutic potential of *Lawsonia inermis* accounted for its traditional use in the treatment of ulcers, jaundice, hair loss, leukoderma, and Malaria, which are attributed to the variety of bioactive compounds present in the herbal plant [17].

However, despite several reports on the antiplasmodial activities of *Lawsonia inermis* Leaves, the mechanism with which the plant inhibits the activity of *P. falciparum* in the human body remains unknown. Fortunately, computational studies (otherwise known as *in silico* studies) provide the opportunity to explore and understand the mechanism of action of phytocompounds present in plants against therapeutic targets and even pathways involved. In this regard, an increasingly used approach is a combination of network pharmacology approach, molecular docking analysis, and molecular dynamics simulation [18, 19]. These approaches help understand, and demonstrate the rationality of phytocompounds in herbal plants, study their interactions with potential drug targets and assess how the interaction between the drug leads and targets will behave within a simulated physiological environment. Additionally, an ADMET profiling of the drug leads can shed light on the pharmacokinetics and chemistry values of the molecules [20], which may give some insights into their economic values.

Thus, this study seeks to use the Gas-chromatography mass-spectrometry technique and various computational approaches, including network pharmacology, molecular docking, ADMET profile and Molecular dynamics simulation, to understand the key bioactive compounds responsible for the antiplasmodial activities of *Lawsonia inermis*, the most influential drug targets, and the pathways through which the antiplasmodial mechanism of action takes place.

Materials and methods

Sample collection and identification

The leaves of *Lawsonia inermis* were retrieved from Oyo town, Oyo State, Nigeria, based on the descriptions in literature and trade-medical practitioners. The fresh samples were taken to the Herbarium unit, Department of Botany, University of Ibadan (UI), for identification purposes. The unit identified the sample as *Lawsonia inermis* and provided the voucher number: UIH-23126.

Preparation of *Lawsonia inermis* leaves and determination of extract yields

The leaves of *Lawsonia inermis* (LIL) were air-dried at normal room temperature (25–27 °C) with proper ventilation for two weeks. At the Grinding room, Department of Chemistry, UI, the dried sample was pulverized, and the powdered sample was kept within a labeled polythene bag. In the experimental laboratory, the LIL sample was put

in a clean flat-bottomed glass container, and Dichloromethane and methanol were added in a ratio of 1: 1 until the solvent covered the sample sufficiently. Across 48 hours, the sample was stirred adequately and covered using foil paper. After 48 hours, the filtrate was collected using filter paper (Whatman No. 1). Each sample's filtrate was concentrated using a rotary evaporator at 35 °C temperature. After the concentration of the samples, they were subjected to drying in a water bath and then hot air oven at room temperature. The crude extract was then used for the characterization of phytocompounds using the Gas chromatography Mass spectrometry (GC-MS) technique. The percentage yield of *Lawsonia inermis* Leaves extract was calculated using the formula below:

$$\text{Percentage yield} = \frac{\text{Weight of final extract}}{\text{Soaked sample material}} \times 100\%$$

Application of Gas Chromatography-Mass Spectrometry Analysis

A Gas chromatography-mass spectrometry approach was used to characterize the phytochemicals present in the prepared leaves extract of *Lawsonia inermis*. The GC Agilent USA (7890A) machine was used by coupling it with a mass spectrophotometer (5975C). This combination included an auto-injector (10ul syringe) and a triple-axis detector, while the helium gas was used as the carrier gas. The specification of the GC-MS condition, capillary column, the temperature of the column, and total elution were set to standards previously reported by [21]. The mass spectrophotometry software was used to control the system and acquire data, which were compared with those available at the National Institute of Standard and Technology (NIST) library.

Collation of identified phytocompounds in leaves extract of *Lawsonia inermis*

The detailed information on the identified phytocompounds in the leaf extract of *Lawsonia inermis* was retrieved from the PubChem database with key values, including molecular weight, molecular formula, and canonical smiles.

Absorption, Distribution, Metabolism, Excretion, and Toxicity & Druglikeness Screening

The retrieved and collated phytocompounds were subjected to absorption, distribution, metabolism, excretion, and toxicity (ADMET) and drug-likeness analysis to reduce attrition rate during further drug discovery and development processes. An open-access online server, AdmetLab 2.0 was used to predict crucial ADMET tests for each phytocompound [22]. For druglikeness assessment of the phytocompound, Lipinski's rule of Five was employed, while Protox II server was used to determine their toxicity class [23].

Collation of *Plasmodium falciparum* Malaria protein targets

Protein targets of *P. falciparum* Malaria were retrieved from multiple databases, including OMIM, GeneCards, and NCBI, using the keywords "Malaria" and "*Plasmodium falciparum*." The Online Venn Diagram tool, Venny 2.0, was used to find any overlapping targets to remove any repetition.

Screening of *Plasmodium falciparum* Genes associated with the *Lawsonia inermis* phytocompounds

The targets of each screened compound, including the standard drugs, namely pyrimethamine and hydroxychloroquine, were predicted across four different databases, namely, BindingDB, SEA, SwissTargetPrediction and SuperPred. The collated genes were cleaned on an Excel sheet, while the Venny 2.0 was also used to find overlapping targets for each compound to determine their putative *P. falciparum* targets.

Development of Protein-Protein Interaction Network

All screened putative genes of the compounds of *Lawsonia inermis* herbal plant Leaves were collated and submitted to the STRING server to develop the Protein-protein interaction network (PPI). The choice of organism and correlation degree were set to "Home sapiens" and ≥ 0.700, respectively. The PPI network provides crucial information, including key targets, Gene ontology and disease-gene association. The network was sent to Cytoscape for further analysis to determine the most essential genes.

Kyoto Encyclopaedia of Genes and Genomes (Kegg) Pathway and Gene Ontology analysis

The KEGG pathway analysis helps link the gene sets to functional information to collate significantly enriched biological pathways that are related to Malaria and its associated symptoms [24]. All Malaria and symptoms-related pathways were retrieved from STRING based on the Protein-protein interaction network of *Lawsonia inermis* Leaves and tabulated for compound-targets-pathways network construction.

Also, the biological processes (BP), molecular function (MF), and cellular component (CC) that constitute the Gene Ontology profiles of the protein targets were assessed by using the Funrich software. The most significant molecular processes, cellular components and biological processes were identified by setting the P value at < 0.05 [25].

Development of Compounds-Targets-Pathways Network

The relationship between the phytocompounds present in the leaf extract of *Lawsonia inermis* and associated protein targets and pathways was developed using Cytoscape 3.10.0 and Java 17.0.5. The software also enables users to visualize and study the interactions by creating the compounds and gene targets and gene targets and enriched pathways as input nodes. The network was analyzed by using the Cyto-Hubba plug-in on Cytoscape to perform Maximal Clique Centrality (MCC) topological analysis [26].

Assessment of Protein-ligand Interaction by Molecular Docking

The phytocompounds from the leaves extract of *Lawsonia inermis* were docked against five *Plasmodium falciparum* Malaria targets identified, namely GSK3β (PDB:5f95), MAPK1 (PDB:4fv9), IDO1 (PDB:5etw), SPHK1 (PDB:4L02) and MMP9 (PDB:1gkc). All the protein targets were downloaded from the protein databank in 3D format. The BIOVIA Discovery Studio 2021 and Chimera 1.14 software were used to prepare the protein targets and add hydrogens [27].

To commence the docking process, the structure data file (SDF) of the phytocompounds and standard drugs (Pyrimethamine and Hydroxychloroquine) were downloaded from the PubChem database. The PyRx software, a virtual screening tool, was initiated with the target uploaded as molecules and the phytocompounds as chemical table files. Embedded in the PyRx tool is the Autodock Vina tool for docking the ligands (Phytocompounds) against each protein target at their specific active sites. The active sites of each protein target were determined on the CASTp 3.0 database. The Vina tool provided the binding affinity score of each ligand interaction against the target. The interaction between each phytocompound and target (known as complex) was visualized and studied using the BIOVIA Discovery Studio 2021.

Assessment of the best complexes by Molecular Dynamics Simulation

The best complexes from previous analysis including the best standard ligand-protein complex, underwent molecular dynamics simulation analysis. This is to assess how stable and flexible the complexes are, which can influence their efficacy if eventually developed. The Schrodinger LLC Desmond Software was used to study the molecular dynamics behavior of the complexes for 100 ns. Upon docking the ligand and protein to establish their static view concerning the binding position of the ligand within the binding pocket of the protein, the simulation was commenced [28]. The classical equation of motion by Newton was employed to calculate the atom displacement across time during the simulation analysis. Thus, it becomes possible to predict the states of binding by the ligands in a physiological environment [29]. A successful complex pre-processing was performed with Protein Preparation Wizard on Maestro, while the System Builder Tool was used to establish the system. Shivakumar et al. had previously reported successful temperature, pressure, and force

field standards of the Intermolecular Interaction Potential 3 Points Transferable solvent model [30], which were applied in this study. Counter ions were used for model neutralization, and NaCl 0.15M was applied for the simulation of physiological conditions. Models were loosened before simulation, and trajectories were stored for inspection after every 100 ps.

Results

Percentage yield of *Lawsonia inermis* leaves extracts

The Dichloromethane-Methanol extract of *Lawsonia inermis* Leaves (LIL) had a low but sufficient yield of 12.39 %.

The outcome of Gas Chromatography-Mass Spectrometry Analysis

A total of 58 phytocompounds were identified from LIL extract, with the retention time and peak area percentage ranging from 2.412 to 18.557 and –0.20 % to 18.46 %, respectively. All the identified phytocompounds in the LIL extract are listed in Table 1.

Adsorption, Distribution, Metabolism, Excretion and Toxicity & Druglikeness Screening

Out of 58 LIL phytocompounds, 12 compounds were predicted to have the most promising ADMET properties, as shown in Figure 1. Only Paromomycin violated more than two of Lipinski's rule of five, as listed in Table 2.

Collation of *Plasmodium falciparum* Malaria Genes

For this study, genes associated with the Malaria pathogen of interest were collated from different databases, including GeneCards (757), OMIM (82), and NCBI (71). Upon placing the genes on Venny 2.0, six hundred and fifty-one, eighteen, and three genes are distinctly found on GeneCards, OMIM and NCBI, respectively, as shown in Figure 2.

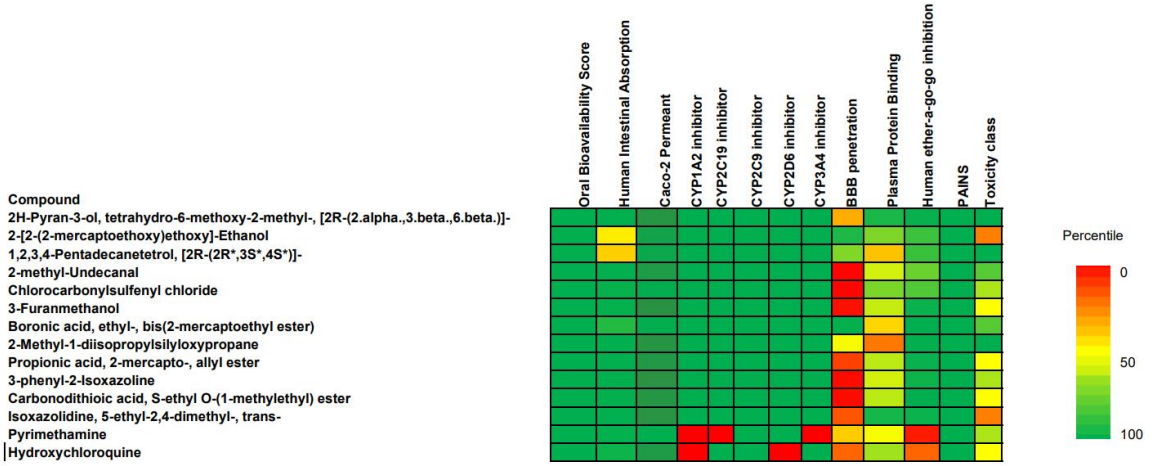

Figure 1 Heatmap showing most promising Phytocompounds of *Lawsonia inermis* Leaves and Standard Drugs (Controls) Based on ADMET Profiling. Green, yellow, and red colours represent good, fair, and poor phytocompound for each parameter.

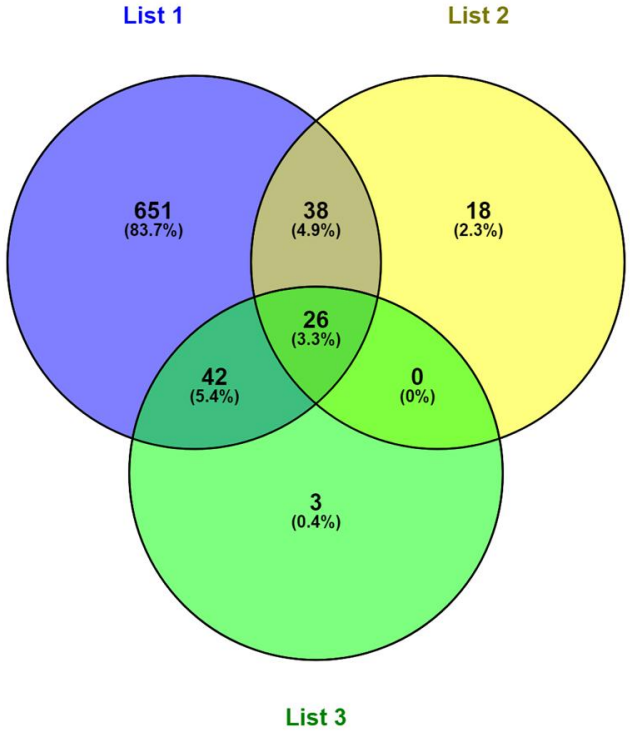

Figure 2 A visual representation of *P. falciparum* malaria targets from three databases, including GeneCards (Blue), OMIM (Yellow), and NCBI (Green) to identify any overlapping genes using Venny 2.0 tool.

Table 1 A summary of Phytocompounds Identified from *Lawsonia inermis* Leaves (LIL) extract with GC-MS technique

S/N	RT	CAS No.	Compounds	PubChem ID	Formular	Molecular Weight (g/mol)
1	2.412	095057-50-4	1-Hydroxy-4-hydrazinocarbonyl-2,2,5,5-tetramethyl-3-imidazoline-3-oxide	135580712	$C_8H_{16}N_4O_3$	216.24
2	2.412	136953-05-4	1,2,3,4-Pentadecanetetrol, [2R-(2R*,3S*,4S*)]-	15120029	$C_{15}H_{32}O_4$	276.41
3	2.412	136953-03-2	1,2,3,4-Tridecanetetrol, [2R-(2R*,3S*,4S*)]-	554092	$C_{13}H_{28}O_4$	248.36
4	3.025	000110-41-8	2-methyl-Undecanal	61031	$C_{12}H_{24}O$	184.32
5	3.025	021317-50-0	2H-Pyran-3-ol, tetrahydro-6-methoxy-2-methyl-, [2R-(2.alpha.,3.beta.,6.beta.)]-	547129	$C_7H_{14}O_3$	146.18
6	3.025	000093-30-1	Methoxyphenamine	4117	$C_{11}H_{17}NO$	179.26
7	3.394	000616-91-1	Acetylcysteine	12035	$C_5H_9NO_3S$	163.2
8	3.394	1000151-82-1	10-Undecen-1-al, 2-methyl-	547085	$C_{12}H_{22}O$	182.3
9	3.394	000498-07-7	.beta.-D-Glucopyranose, 1,6-anhydro-	2724705	$C_6H_{10}O_5$	162.14
10	3.62	1000256-18-9	N-[3-Methylaminopropyl]aziridine	547048	$C_6H_{14}N_2$	114.19
11	3.62	099985-55-4	2-Dimethylamino-3'-methoxyacetophenone	546935	$C_{11}H_{15}NO_2$	193.24
12	4.27	000930-27-8	3-methyl-Furan	13587	C_5H_6O	82.1
13	4.27	088787-23-9	Cyclopropanecarboxylic acid, 2-methylene-, methyl ester	543056	$C_6H_8O_2$	112.13
14	4.27	1000130-96-4	7-Methyl-Z-8,10-dodecadienal	5363533	$C_{13}H_{22}O$	194.31
15	4.645	042513-42-8	8-Dodecenol	5364469	$C_{12}H_{24}O$	184.32
16	4.645	075039-84-8	trans-2-Undecen-1-ol	5365004	$C_{11}H_{22}O$	170.29
17	4.927	070569-68-5	Chloro-methyl-methoxy-amine	548183	C_2H_6ClNO	95.53
18	4.927	002757-23-5	Chlorocarbonylsulfenyl chloride	75990	CCl_2OS	130.979
19	5.928	004412-91-3	3-Furanmethanol	20449	$C_5H_6O_2$	98.1
20	5.928	074752-93-5	1,1,2,3-tetramethyl-Cyclopropane	544034	C_7H_{14}	98.19
21	8.624	002319-57-5	1,2,3,4-Butanetetrol, [S-(R*,R*)]-	8998	$C_4H_{10}O_4$	122.12
22	8.624	1000161-44-5	Boronic acid, ethyl-, bis(2-mercaptoethyl ester)	548364	$C_6H_{15}BO_2S_2$	194.1
23	8.624	1000279-16-9	2-Methyl-1-diisopropylsilyloxypropane	6329048	$C_{10}H_{23}OSi$	187.37
24	9.199	000488-81-3	Ribitol	6912	$C_5H_{12}O_5$	152.15
25	9.199	056282-36-1	2-[2-(2-mercaptoethoxy)ethoxy]-Ethanol	548394	$C_6H_{14}O_3S$	166.24
26	9.806	016883-50-4	Propionic acid, 2-mercapto-, allyl ester	548368	$C_6H_{10}O_2S$	146.21
27	9.806	052317-55-2	1,1-Bis(methylthio)pentane	548396	$C_7H_{16}S_2$	164.3
28	9.806	002782-07-2	D-Galactonic acid,.gamma.-lactone	608	$C_6H_{10}O_6$	178.14
29	10.213	007542-37-2	Paromomycin	165580	$C_{23}H_{45}N_5O_{14}$	615.6
30	10.213	068832-18-8	1-Deoxy-d-altritol	18667263	$C_6H_{14}O_5$	166.17
31	10.644	076003-39-9	3-ethylidene-2-methyl-1-Hexen-4-yne	534155	C_9H_{12}	120.19
32	10.644	000876-02-8	4-Hydroxy-3-methylacetophenone	70135	$C_9H_{10}O_2$	150.17
33	11.138	1000157-99-5	3-phenyl-2-Isoxazoline	840162	C_9H_9NO	147.17
34	11.138	038379-93-0	Carbonodithioic acid, S-ethyl O-(1-methylethyl) ester	539987	$C_6H_{12}OS_2$	164.3
35	11.658	1000130-08-6	3-Methylmannoside	247323	$C_7H_{14}O_6$	194.18
36	11.658	000111-82-0	Dodecanoic acid, methyl ester	8139	$C_{13}H_{26}O_2$	214.34
37	11.658	005129-56-6	Undecanoic acid, 10-methyl-, methyl ester	554144	$C_{13}H_{26}O_2$	214.34
38	12.927	000709-50-2	.beta.-D-Glucopyranoside, methyl	91730338	$C_{32}H_{34}O_{14}$	642.6
39	12.927	073367-80-3	12-Bromododecanoic acid	175468	$C_{12}H_{23}BrO_2$	279.21

Table 1 A summary of Phytocompounds Identified from *Lawsonia inermis* Leaves (LIL) extract with GC-MS technique (continue)

S/N	RT	CAS No.	Compounds	PubChem ID	Formular	Molecular Weight (g/mol)
40	12.927	056728-14-4	Isoxazolidine, 5-ethyl-2,4-dimethyl-, trans-	22212546	$C_7H_{15}NO$	129.199
41	13.472	000057-10-3	n-Hexadecanoic acid	985	$C_{16}H_{32}O_2$	256.42
42	13.472	000544-63-8	Tetradecanoic acid	11005	$C_{14}H_{28}O_2$	228.37
43	13.472	000057-11-4	Octadecanoic acid	5281	$C_{18}H_{36}O_2$	284.5
44	13.978	013481-95-3	10-Octadecenoic acid, methyl ester	12559718	$C_{19}H_{36}O_3$	312.5
45	13.978	1000333-58-3	cis-13-Octadecenoic acid, methyl ester	12541027	$C_{19}H_{36}O_2$	296.5
46	13.978	001937-63-9	11-Octadecenoic acid, methyl ester, (Z)-	5364505	$C_{19}H_{36}O_2$	296.5
47	14.466	000112-80-1	Oleic Acid	445639	$C_{18}H_{34}O_2$	282.5
48	14.466	1000130-90-5	2-Methyl-Z,Z-3,13-octadecadienol	5364412	$C_{19}H_{36}O$	280.5
49	14.973	003443-84-3	9-Octadecenoic acid (Z)-, 2-hydroxy-1-(hydroxymethyl)ethy l ester	5319879	$C_{21}H_{40}O_4$	356.5
50	14.973	1000131-33-2	Z-(13,14-Epoxy)tetradec-11-en-1-ol acetate	5363633	$C_{16}H_{28}O_3$	268.39
51	15.98	018633-25-5	Oxirane, tridecyl-	86768	$C_{15}H_{30}O$	226.4
52	15.98	000112-86-7	Erucic acid	5281116	$C_{22}H_{42}O_2$	338.6
53	16.512	000111-03-5	9-Octadecenoic acid (Z)-, 2,3-dihydroxypropyl ester	5283468	$C_{21}H_40O_4$	356.5
54	16.512	1000130-90-5	2-Methyl-Z,Z-3,13-octadecadienol	5364412	$C_{19}H_{36}O$	280.5
55	17.763	052207-99-5	cis-7,cis-11-Hexadecadien-1-yl acetate	5363265	$C_{18}H_{32}O_2$	280.4
56	17.763	1000336-71-7	n-Propyl 11-octadecenoate	87131822	$C_{21}H_{40}O_2$	324.5
57	18.557	1000130-90-5	2-Methyl-Z,Z-3,13-octadecadienol	5364412	$C_{19}H_{36}O$	280.5
58	18.557	058594-45-9	(Z)-13-Octadecenal	5364497	$C_{18}H_{34}O$	266.5

Table 2 A summary of the druglikeness properties of *Lawsonia inermis* Leaves compounds and controls based on Lipinski's rule of five

S/N	Compounds	Molecular Formular	Molecular Weight (g/mol)	HBD	HBA	iLOGP	Lipinski's Violation
1	1-Hydroxy-4-hydrazinocarbonyl-2,2,5,5-te tramethyl-3-imidazoline-3-oxide	$C_8H_{16}N_4O_3$	216.24	3	5	1.28	0
2	1,2,3,4-Pentadecanetetrol, [2R-(2R*,3S*,4S*)]-	$C_{15}H_{32}O_4$	276.41	4	4	3.29	0
3	1,2,3,4-Tridecanetetrol, [2R-(2R*,3S*,4S*)]-	$C_{13}H_{28}O_4$	248.36	4	4	2.8	0
4	2-methyl-Undecanal	$C_{12}H_{24}O$	184.32	0	1	3.16	0
5	2H-Pyran-3-ol, tetrahydro-6-methoxy-2-methyl-, [2R-(2.alpha.,3.beta.,6.beta.)]-	$C_7H_{14}O_3$	146.18	1	3	1.85	0
6	Methoxyphenamine	$C_{11}H_{17}NO$	179.26	1	2	2.59	0
7	Acetylcysteine	$C_5H_9NO_3S$	163.19	2	3	0.65	0
8	10-Undecen-1-al, 2-methyl-	$C_{12}H_{22}O$	182.3	0	1	3.02	0
9	.beta.-D-Glucopyranose, 1,6-anhydro-	$C_6H_{10}O_5$	162.14	3	5	1.27	0
10	N-[3-Methylaminopropyl]aziridine	$C_6H_{14}N_2$	114.19	1	2	1.91	0
11	2-Dimethylamino-3'-methoxyacetophenon e	$C_{11}H_{15}NO_2$	193.24	0	3	2.2	0
12	3-methyl-Furan	C_5H_6O	82.1	0	1	1.68	0
13	Cyclopropanecarboxylic acid, 2-methylene-, methyl ester	$C_6H_8O_2$	112.13	0	2	1.94	0
14	7-Methyl-Z-8,10-dodecadienal	$C_{13}H_{22}O$	194.31	0	1	3.16	0
15	8-Dodecenol	$C_{12}H_{24}O$	184.32	1	1	3.45	0
16	trans-2-Undecen-1-ol	$C_{11}H_{22}O$	170.29	1	1	3.12	0
17	Chloro-methyl-methoxy-amine	C_2H_6ClNO	95.53	0	2	1.79	0
18	Chlorocarbonylsulfenyl chloride	CCl_2OS	130.98	0	1	1.43	0

Table 2 A summary of the druglikeness properties of *Lawsonia inermis* Leaves compounds and controls based on Lipinski's rule of five (continue)

S/N	Compounds	Molecular Formular	Molecular Weight (g/mol)	HBD	HBA	iLOGP	Lipinski's Violation
19	3-Furanmethanol	$C_5H_6O_2$	98.1	1	2	1.4	0
20	1,1,2,3-tetramethyl-Cyclopropane	C_7H_{14}	98.19	0	0	2.37	0
21	1,2,3,4-Butanetetrol, [S-(R*,R*)]-	$C_4H_{10}O_4$	122.12	4	4	0.61	0
22	Boronic acid, ethyl-, bis(2-mercaptoethyl ester)	$C_6H_{15}BO_2S_2$	194.12	0	2	0	0
23	2-Methyl-1-diisopropylsilyloxypropane	$C_{10}H_{23}OSi$	187.37	0	1	3.39	0
24	Ribitol	$C_5H_{12}O_5$	152.15	5	5	0.56	0
25	2-[2-(2-mercaptoethoxy)ethoxy]-Ethanol	$C_6H_{14}O_3S$	166.24	1	3	1.89	0
26	Propionic acid, 2-mercapto-, allyl ester	$C_6H_{10}O_2S$	146.21	0	2	1.96	0
27	1,1-Bis(methylthio)pentane	$C_7H_{16}S_2$	164.33	0	0	2.59	0
28	D-Galactonic acid,.gamma.-lactone	$C_6H_{10}O_6$	178.14	4	6	0.11	0
29	Paromomycin	$C_{23}H_{45}N_5O_{14}$	615.63	13	19	0.69	3
30	1-Deoxy-d-altritol	$C_6H_{14}O_5$	166.17	5	5	0.47	0
31	3-ethylidene-2-methyl-1-Hexen-4-yne	C_9H_{12}	120.19	0	0	2.68	0
32	4-Hydroxy-3-methylacetophenone	$C_9H_{10}O_2$	150.17	1	2	1.54	0
33	3-phenyl-2-Isoxazoline	C_9H_9NO	147.17	0	2	1.77	0
34	Carbonodithioic acid, S-ethyl O-(1-methylethyl) ester	$C_6H_{12}OS_2$	164.29	0	1	2.56	0
35	3-Methylmannoside	$C_7H_{14}O_6$	194.18	4	6	1.08	0
36	Dodecanoic acid, methyl ester	$C_{13}H_{26}O_2$	214.34	0	2	3.48	0
37	Undecanoic acid, 10-methyl-, methyl ester	$C_{13}H_{26}O_2$	214.34	0	2	3.69	0
38	.beta.-D-Glucopyranoside, methyl	$C_7H_{14}O_6$	194.18	4	6	1.25	0
39	12-Bromododecanoic acid	$C_{12}H_{23}BrO_2$	279.21	1	2	3.12	0
40	Isoxazolidine, 5-ethyl-2,4-dimethyl-, trans-	$C_7H_{15}NO$	129.2	0	2	2.31	0
41	n-Hexadecanoic acid	$C_{16}H_{32}O_2$	256.42	1	2	3.85	1
42	Tetradecanoic acid	$C_{14}H_{28}O_2$	228.37	1	2	3.32	0
43	Octadecanoic acid	$C_{18}H_{36}O_2$	284.48	1	2	4.3	1
44	10-Octadecenoic acid, methyl ester	$C_{19}H_{36}O_2$	296.49	0	2	4.69	1
45	cis-13-Octadecenoic acid, methyl ester	$C_{19}H_{36}O_2$	296.49	0	2	4.77	1
46	11-Octadecenoic acid, methyl ester, (Z)-	$C_{19}H_{36}O_2$	296.49	0	2	4.79	1
47	Oleic Acid	$C_{18}H_{34}O_2$	282.46	1	2	4.27	1
48	2-Methyl-Z,Z-3,13-octadecadienol	$C_{19}H_{36}O$	280.49	1	1	4.96	1
49	2-octyl-Cyclopropaneoctanal	$C_{19}H_{36}O$	280.49	0	1	4.56	1
50	9-Octadecenoic acid (Z)-, 2-hydroxy-1-(hydroxymethyl)ethyl ester	$C_{21}H_{40}O_4$	356.54	2	4	4.65	0
51	Z-(13,14-Epoxy)tetradec-11-en-1-ol acetate	$C_{16}H_{28}O_3$	268.39	0	3	3.8	0
52	Oxirane, tridecyl-	$C_{15}H_{30}O$	226.4	0	1	4.27	0
53	Erucic acid	$C_{22}H_{42}O_2$	338.57	1	2	5.22	1
54	9-Octadecenoic acid (Z)-, 2,3-dihydroxypropyl ester	$C_{21}H_{40}O_4$	356.54	2	4	4.33	0
55	2-Methyl-Z,Z-3,13-octadecadienol	$C_{19}H_{36}O$	280.49	1	1	4.96	1
56	cis-7,cis-11-Hexadecadien-1-yl acetate	$C_{18}H_{32}O_2$	280.45	0	2	4.52	1
57	n-Propyl 11-octadecenoate	$C_{21}H_{40}O_2$	324.54	0	2	5.32	1
58	2-Methyl-Z,Z-3,13-octadecadienol	$C_{19}H_{36}O$	280.49	1	1	4.96	1
59	(Z)-13-Octadecenal	$C_{18}H_{34}O$	266.46	0	1	4.47	1
60	Pyrimethamine	$CCC_1 = C(C(= NC(= N1)N)N)C_2 = CC = C(C = C_2)Cl$	248.08	4	4	1.179	0
61	Hydroxychloroquine	$CCN(CCCC(C)NC_1 = C_2C = CC(= CC_2 = NC = C_1)Cl)CCO$	335.18	2	4	3.696	0

Note: HBD means number of Hydrogen Bond Donors; HBA means number of Hydrogen Bond Acceptors; and iLogP means logarithm of the n-octanol/water distribution coefficient.

Prediction and collation of *Plasmodium falciparum* Malaria Genes of the *Lawsonia inermis* Phytocompounds

The putative targets of the successful *Lawsonia inermis* Leave (LIL) phytocompounds from ADMET and druglikeness screening were retrieved from Swiss Target Prediction, BindingDB, and SEA databases and collated for further studies as shown in Table 3.

The outcome of Protein-protein Interaction (PPI) Network Analysis

The protein-protein interaction network of Malaria proteins based on genes from *Lawsonia inermis* Leaves phytocompounds is shown in Figure 3. The network was subjected to Maximal Clique Centrality (MCC) topological analysis, and SRC, HSP90AA1, CXCR4, TL4, MMP9, VEGFA, NOS3, ADRB2, F2, and ITGB3 are the most essential proteins in LIL PPI network as shown Figure 4.

The outcome of Kyoto Encyclopaedia of Genes and Genomes (KEGG) Pathway and Gene Ontology Analysis

The Gene ontology analysis included ninety-four genes for LIL phytocompounds. The functional enrichment analysis of the genes showed that they are significantly enriched in 231 cellular components (CC), 407 molecular functions (MF) and 1636 biological processes (BP). Figure 5 (A-C) shows the top eight statistically significant molecular functions, biological processes, and cellular components.

The KEGG pathway analysis identified forty-one pathways as potentially involved in the antimalarial activity of phytocompounds in the *Lawsonia inermis* plant, as listed in Table 4. Metabolic pathways (27), PI3K-Akt signaling pathway (12), and HIF-1 signaling pathway (10) are found to be the top 3 pathways involved in the antimalarial activities of LIL compounds.

Compound-target-pathway network of *Lawsonia inermis* leaves (LIL)

The CTP network of LIL consisted of one hundred and twenty-four (124) nodes and three hundred and sixty-six edges with a network diameter (largest distance between two nodes) of 6mm while the average number of neighbors is 5.903 (Figure 6). Using the cytohubba plugin, maximal clique centrality (MCC) topological analysis revealed that Mitogen-Activated Protein Kinase 1 (MAPK1), Proto-oncogene tyrosine-protein kinase (SRC) and Platelet-derived growth factor receptor β (PDGFRβ) are the top three most essential targets in the network with the highest number of interactions while metabolic pathways, PI3K-Akt signaling pathway, and HIF-1 signaling pathway are the top three pathways that modulated the highest number of proteins. Also, 2-[2-(2-mercapto ethoxy) ethoxy]-Ethanol, Boronic acid ethyl-bis(2-mercaptoethanol ester) and Chlorocarbonylsulfenyl chloride are the essential compounds in the network.

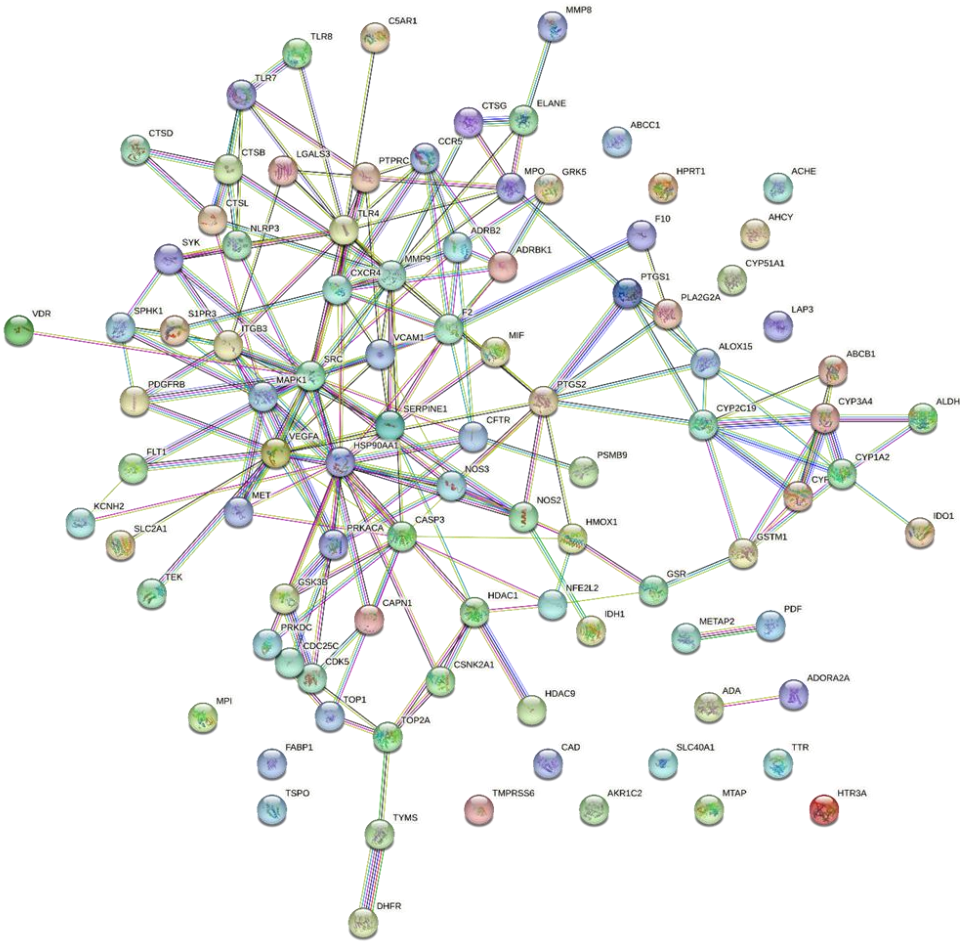

Figure 3 Protein-protein interaction network of Malaria protein targets by bioactive compounds of *Lawsonia inermis* (Leaves). Network nodes (circle) represents the proteins with coloured nodes standing for query proteins and first shell of interactors and white nodes for second shell of interactors. All nodes are filled, suggesting that the 3D structure is known or predicted. Network edges (lines) represent protein-protein associations with light blue edges standing for known interactions from curated databases and pink standing for experimentally determined associations. Predicted interactions are represented by green, red, and blue colours, suggesting gene neighbourhood, gene fusions and gene co-occurrence, respectively. Other edge colours, including yellow, black, and light blue, represents text mining, co-expression, and protein homology, respectively.

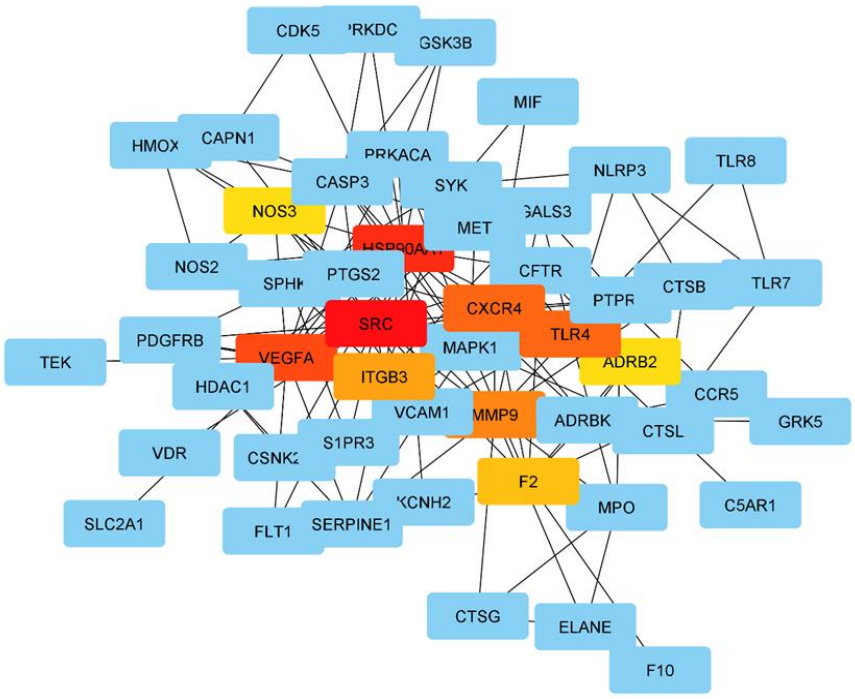

Figure 4 A sub-network showing top 10 frequently implicated protein targets based on Maximal Clique Centrality (MCC) topological analysis of PPI network of Malaria proteins by bioactive compounds of *Lawsonia inermis* (Leaves). The top 10 essential proteins in the PPI network are represented by red, pink, brown and yellow colours. The colour spectrum from red to yellow indicates the most essential proteins to the least essential proteins among the ten.

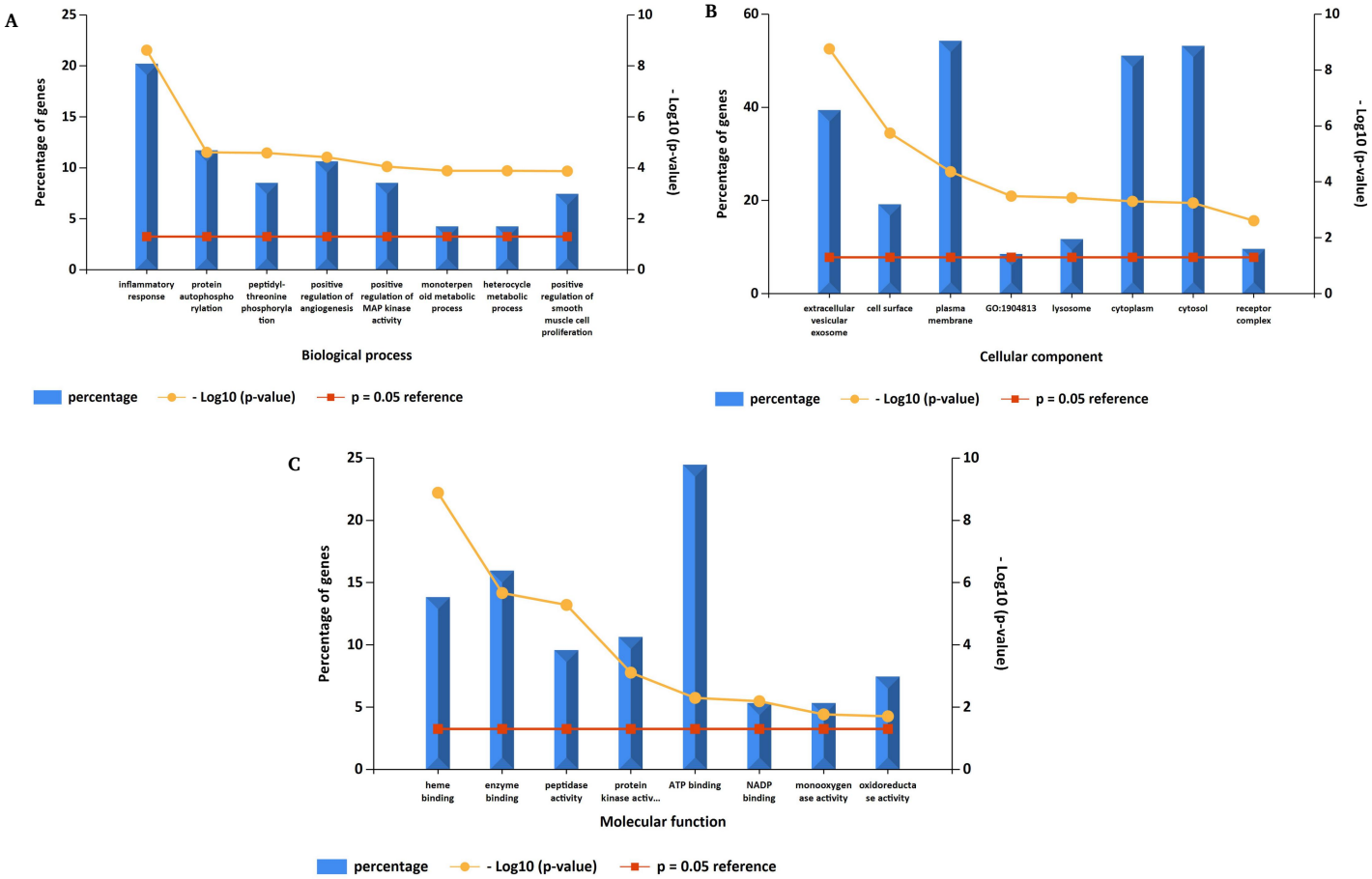

Figure 5 Top 8 enriched (A) Biological Processes (B) Cellular components (C) molecular functions by *L. inermis* (Leaves) compounds' genes based on Gene Ontology Analysis (*P* value < 0.05 was considered as statistically significant for gene enrichment).

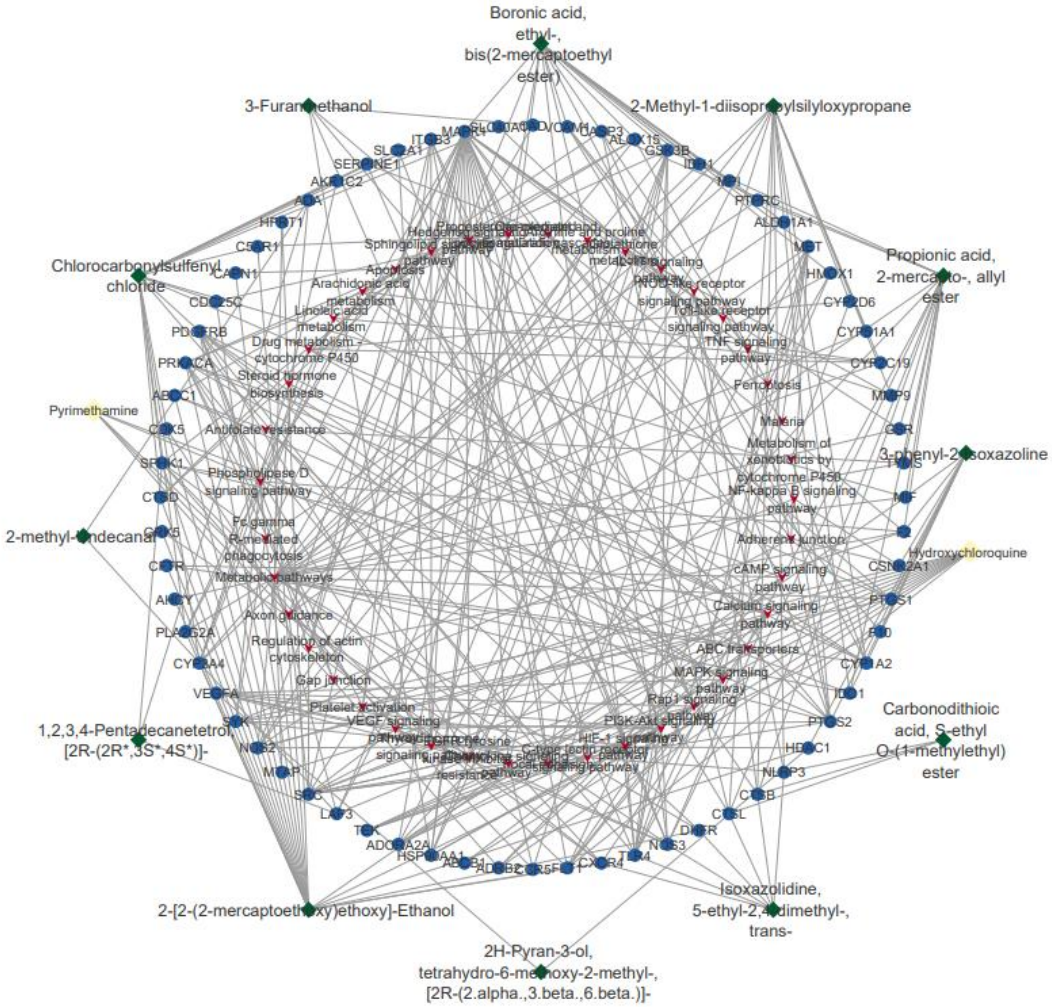

Figure 6 A network construction showing the interaction among bioactive compounds of *L. inermis* (Leaves), their malaria-related targets and associated pathways. The green nodes represent the compounds; the blue nodes represent the targets (proteins); the red nodes represent the associated pathways; Standard drugs are identified in yellow nodes. The line is the edge that represent the interactions.

Table 3 Phytocompounds of *Lawsonia inermis* Leaves and standard drugs with their putative Malaria

Compound	Targets
2H-Pyran-3-ol, tetrahydro-6-methoxy-2-methyl-, [2R-(2.alpha.,3.beta.,6.beta.)]-	VEGFA, LGALS3, HDAC9, HDAC1
2-[2-(2-mercaptoethoxy)ethoxy]-Ethanol	NFE2L2, VDR, LGALS3, AHCY, CFTR, TTR, CXCR4, DHFR, MIF, CYP3A4, PLA2G2A, GRK5, METAP2, CTSD, SPHK1, CDK5, ABCC1, PRKACA, HDAC9, F10, PDGFRB, TOP1, CDC25C, SLC40A1, FLT1, CAPN1, C5AR1, HPRT1, S1PR3, HDAC1
1,2,3,4-Pentadecanetetrol, [2R-(2R*,3S*,4S*)]-	LAP3, SPHK1, ADA
2-methyl-Undecanal	LAP3, PDF, ADA
Chlorocarbonylsulfenyl chloride	MIF, AKR1C2, CYP3A4, PLA2G2A, NFE2L2, SERPINE1, PTGS1, SLC2A1, METAP2, CTSD, SPHK1, CDK5, ITGB3, HTR3A, PSMB9, PDGFRB, MAPK1, TMPRSS6, CDC25C, SLC40A1, TLR4, C5AR1
3-Furanmethanol	HSP90AA1, PTGS1, CAD, TLR4, PTGS2
Boronic acid, ethyl-, bis(2-mercaptoethyl ester)	VCAM1, ELANE, HSP90AA1, ADORA2A, CASP3, ALOX15, GSK3B, HTR3A, IDH1, MPI, PTPRC, CYP1A2, ALDH1A1, MAPK1, CTSL, MET, TLR4, HMOX1, NOS2
2-Methyl-1-diisopropylsilyloxypropane	CYP2D6, MPO, ADORA2A, CYP3A4, ACHE, NLRP3, CTSB, CYP51A1, TSPO, CYP1A2, CTSL, IDO1, CCR5, NOS2, CYP2C19, MMP9, PTGS2
Propionic acid, 2-mercapto-, allyl ester	MIF, GSR, ELANE, TYMS, F2, NOS3, ADORA2A, CASP3, ACHE, CTSG, METAP2, GSK3B, CTSB, PTPRC, FABP1, CTSL, TLR4, IDO1, NOS2
3-phenyl-2-Isoxazoline	MIF, F2, CSNK2A1, ACHE, PTGS1, F10, CYP1A2, GRK2, IDO1, PTGS2, HDAC1
Carbonodithioic acid, S-ethyl O-(1-methylethyl) ester	ACHE, NLRP3, CTSB, CTSL
Isoxazolidine, 5-ethyl-2,4-dimethyl-, trans-	DHFR, NOS3, ACHE, NLRP3, CXCR4, CTSB, CTSL, TLR4
*Pyrimethamine	PDGFRB, ALDH1A1, CYP2D6, ELANE, DHFR, NOS3, F2, ACHE, MIF, NOS2, KCNH2
*Hydroxychloroquine	SPHK1, HTR3A, CYP2D6, NOS3, ACHE, PTGS2, HSP90AA1, NOS2, ABCB1, ADRB2, SRC, KCNH2

Table 4 List of modulated malaria pathways enriched by *Lawsonia inermis* (Leaves) gene sets

S/N	ID	Pathways	Gene count	Gene Code
1	hsa04066	HIF-1 signalling pathway	10	MAPK1, HMOX1, SERPINE1, FLT1, NOS3, NOS2, TLR4, TEK, SLC2A1, VEGFA
2	hsa04020	Calcium signalling pathway	8	PDGFRB, NOS3, ADRB2, PRKACA, SPHK1, NOS2, ADORA2A, CXCR4
3	hsa00591	Linoleic acid metabolism	5	CYP3A4, CYP1A2, CYP2C19, PLA2G2A, ALOX15
4	hsa04611	Platelet activation	8	MAPK1, NOS3, F2, PRKACA, PTGS1, SRC, SYK, ITGB3
5	hsa04370	VEGF signalling pathway	6	MAPK1, NOS3, SPHK1, PTGS2, SRC, VEGFA
6	hsa04151	PI3K-Akt signalling pathway	12	MAPK1, PDGFRB, FLT1, NOS3, MET, GSK3B, HSP90AA1, TLR4, SYK, TEK, ITGB3, VEGFA
7	hsa01521	EGFR tyrosine kinase inhibitor resistance	6	MAPK1, PDGFRB, MET, GSK3B, SRC, VEGFA
8	hsa04015	Rap1 signalling pathway	9	MAPK1, PDGFRB, FLT1, MET, ADORA2A, SRC, TEK, ITGB3, VEGFA
9	hsa04919	Thyroid hormone signalling pathway	7	MAPK1, PRKACA, GSK3B, HDAC1, SRC, SLC2A1, ITGB3
10	hsa04657	IL-17 signalling pathway	6	MAPK1, CASP3, GSK3B, HSP90AA1, PTGS2, MMP9
11	hsa04062	Chemokine signalling pathway	8	MAPK1, CCR5, PRKACA, ADRBK1, GSK3B, SRC, GRK5, CXCR4
12	hsa00590	Arachidonic acid metabolism	5	PTGS1, PTGS2, CYP2C19, PLA2G2A, ALOX15
13	hsa04510	Focal adhesion	8	MAPK1, PDGFRB, FLT1, MET, GSK3B, SRC, ITGB3, VEGFA
14	hsa00982	Drug metabolism - cytochrome P450	5	GSTM1, CYP3A4, CYP1A2, CYP2D6, CYP2C19
15	hsa01100	Metabolic pathways	27	CYP51A1, MIF, HMOX1, AHCY, GSR, LAP3, CAD, NOS3, ALDH1A1, HPRT1, GSTM1, SPHK1, TYMS, MPI, NOS2, CYP3A4, CYP1A2, PTGS1, PTGS2, CYP2C19, ADA, MTAP, PLA2G2A, IDH1, DHFR, IDO1, ALOX15
16	hsa04071	Sphingolipid signalling pathway	6	MAPK1, CTSD, NOS3, SPHK1, S1PR3, ABCC1
17	hsa04210	Apoptosis	6	MAPK1, CTSD, CASP3, CTSL, CTSB, CAPN1
18	hsa00480	Glutathione metabolism	4	GSR, LAP3, GSTM1, IDH1
19	hsa04625	C-type lectin receptor signalling pathway	5	MAPK1, NLRP3, PTGS2, SRC, SYK
20	hsa04064	NF-kappa B signalling pathway	5	CSNK2A1, VCAM1, PTGS2, TLR4, SYK
21	hsa04668	TNF signalling pathway	5	MAPK1, VCAM1, CASP3, PTGS2, MMP9
22	hsa04010	MAPK signalling pathway	8	MAPK1, PDGFRB, FLT1, PRKACA, CASP3, MET, TEK, VEGFA
23	hsa04520	Adherens junction	4	MAPK1, CSNK2A1, MET, SRC
24	hsa01523	Antifolate resistance	3	TYMS, ABCC1, DHFR
25	hsa04360	Axon guidance	6	MAPK1, MET, GSK3B, SRC, CXCR4, CDK5
26	hsa04610	Complement and coagulation cascades	4	SERPINE1, F2, C5AR1, F10
27	hsa04540	Gap junction	4	MAPK1, PDGFRB, PRKACA, SRC
28	hsa04216	Ferroptosis	3	
29	hsa04072	Phospholipase D signalling pathway	5	MAPK1, PDGFRB, F2, SPHK1, SYK
30	hsa02010	ABC transporters	3	CFTR, ABCC1, ABCB1
31	hsa04666	Fc gamma R-mediated phagocytosis	4	MAPK1, SPHK1, SYK, PTPRC
32	hsa04914	Progesterone-mediated oocyte maturation	4	MAPK1, PRKACA, CDC25C, HSP90AA1
33	hsa04620	Toll-like receptor signalling pathway	4	MAPK1, TLR8, TLR4, TLR7
34	hsa00330	Arginine and proline metabolism	3	LAP3, NOS3, NOS2
35	hsa05144	Malaria	3	VCAM1, MET, TLR4
36	hsa04024	cAMP signalling pathway	5	CFTR, MAPK1, ADRB2, PRKACA, ADORA2A
37	hsa00140	Steroid hormone biosynthesis	3	CYP3A4, CYP1A2, AKR1C2
38	hsa04340	Hedgehog signalling pathway	3	PRKACA, ADRBK1, GSK3B
39	hsa04621	NOD-like receptor signalling pathway	5	MAPK1, HSP90AA1, NLRP3, CTSB, TLR4
40	hsa04810	Regulation of actin cytoskeleton	6	MAPK1, PDGFRB, F2, SRC, CXCR4, ITGB3
41	hsa00980	Metabolism of xenobiotics by cytochrome P450	4	GSTM1, CYP3A4, CYP1A2, CYP2D6

The outcome of Molecular Docking Analysis

The compounds interacted with the selected targets with varying binding affinities, as listed in Table 5. Out of the 48 compounds, only beta.-D-Glucopyranoside, methyl, and Paromomycin have lower binding affinity compared to the standard drugs against GSK3B. The 2-Methyl-Z, Z-3,13-octadecadienol showed a lesser binding affinity against IDO1 compared to Pyrimethamine, while only Paromomycin has a lower binding affinity against the same target compared to both standard drugs. As for MAPK1, none of the phytocompounds from LIL have a lower binding affinity against the target when compared to the standard drugs. Hydroxychloroquine has the least binding affinity not only against MMP9 but also when compared to other drug targets. Hence, it was selected as the control for subsequent studies. Meanwhile, 2-Dimethylamino-3'-methoxyacetophenone and 3-phenyl-2-Isoxazoline have significantly low binding affinity against MMP9 at –7.0 kcal/mol and –7.3 kcal/mol, respectively. Only Paromomycin has a lower binding affinity against SPHK1 compared to the standard drugs. However, 2-Methyl-Z, Z-3,13-octadecadienol has a significantly low binding affinity against the target as well at –7.3 kcal/mol. Consequently, Figure 7 (A-D) shows the two-dimensional (2D) and three-dimensional (3D) visuals of the molecular interactions of the three best complexes based on ADMET profiling, hydrogen carbon interaction, absence of unfavorable bond and least binding affinity score, namely MMP9-2-Dimethylamino-3'-methoxyacetophenone, MMP9-3-phenyl-2-Isoxazoline, and SPHK1-2-Methyl-Z, Z-3,13-octadecadienol, as well as the best standard ligand-protein complex, namely MMP9-Hydroxychloroquine.

Table 5 List of Binding Affinities of *Lawsonia inermis* (Leaves) compounds against selected malaria targets

Compounds	PubChem CID	Binding Affinity (Kcal/mol)				
		GSK3B	IDO1	MAPK1	MMP9	SPHK1
2H-Pyran-3-ol, tetrahydro-6-methoxy-2-methyl-, [2R-(2.alpha.,3.beta.,6.beta.)]-	547129	–6.4	–5	–5.4	–5.8	–5.1
2-[2-(2-mercaptoethoxy)ethoxy]-Ethanol	548394	–3.6	–4.6	–3.6	–4.3	–3.7
1,2,3,4-Pentadecanetetrol, [2R-(2R*,3S*,4S*)]-	554094	–5.6	–5.9	–5	–7	–5.6
2-methyl-Undecanal	61031	–5.1	–5.6	–5.1	–6	–4.6
Chlorocarbonylsulfenyl chloride	75990	–3.5	–3.3	–3.3	–3.4	–3.2
3-Furanmethanol	20449	–4.6	–4.3	–4.3	–4.6	–4.3
Propionic acid, 2-mercapto-, allyl ester	548368	–4	–3.9	–4.2	–4.6	–3.8
3-phenyl-2-Isoxazoline	840162	–6.4	–6.7	–5.7	–7.3	–6.4
Carbonodithioic acid, S-ethyl O-(1-methylethyl) ester	539987	–3.8	–4.2	–3.6	–4.7	–4.2
Isoxazolidine, 5-ethyl-2,4-dimethyl-, trans-	22212546	–4.5	–5.4	–4.8	–5.3	–4.9
1-Hydroxy-4-hydrazinocarbonyl-2,2,5,5-tetramethyl-3-imidazoline-3-oxide	135580712	–5.9	–6.6	–6.2	–5.6	–6.2
1,2,3,4-Tridecanetetrol, [2R-(2R*,3S*,4S*)]-	554092	–5.5	–6.1	–5.2	–6.8	–6
Methoxyphenamine	4117	–5.7	–6.7	–5.5	–6.3	–5.6
Acetylcysteine	12035	–4.7	–4.7	–4.9	–5.2	–4.8
10-Undecen-1-al, 2-methyl-	547085	–4.9	–6.5	–5.1	–5.9	–6.1
.beta.-D-Glucopyranose, 1,6-anhydro-	2724705	–7	–5.3	–4.8	–5.2	–5.4
N-[3-Methylaminopropyl]aziridine	547048	–3.7	–3.9	–3.4	–4.4	–3.9
2-Dimethylamino-3'-methoxyacetophenone	546935	–6	–6.3	–5.8	–7	–5.8
3-methyl-Furan	13587	–4.1	–4.3	–4.1	–4.5	–4.2
Cyclopropanecarboxylic acid, 2-methylene-, methyl ester	543056	–4.9	–4.8	–5	–4.9	–4.8
7-Methyl-Z-8,10-dodecadienal	5363533	–5.2	–6.7	–5.3	–6.4	–6.6
8-Dodecenol	5364469	–5	–6.6	–5.1	–6	–5.9
trans-2-Undecen-1-ol	5365004	–5.1	–6.2	–4.8	–6.1	–5.8
Chloro-methyl-methoxy-amine	548183	–3.5	–3.4	–3.3	–3.6	–3.4
Chlorocarbonylsulfenyl chloride	75990	–3.4	–3.4	–3.3	–3.5	–3.3
1,1,2,3-tetramethyl-Cyclopropane	544034	–4.4	–5.5	–4.2	–4.4	–4.8
1,2,3,4-Butanetetrol, [S-(R*,R*)]-	8998	–4.9	–4.3	–4.2	–4.6	–4.6
Ribitol	6912	–4.7	–4.9	–4.3	–5.3	–5.1
1,1-Bis(methylthio)pentane	548396	–3.7	–4.6	–3.8	–4.3	–4.2
D-Galactonic acid,.gamma.-lactone	608	–7.2	–5.7	–5.2	–6.3	–5.5
Paromomycin	165580	–7.8	–8.4	–7	–5.7	–7.9
1-Deoxy-d-altritol	18667263	–5.1	–4.8	–4.6	–5.8	–5.1
3-ethylidene-2-methyl-1-Hexen-4-yne	534155	–5.3	–6.2	–5	–5.6	–6
4-Hydroxy-3-methylacetophenone	70135	–6.6	–6.5	–6.3	–6.9	–6.7
3-Methylmannoside	247323	–7	–5.9	–5.4	–6	–6
Dodecanoic acid, methyl ester	8139	–4.7	–5.7	–4.9	–6	–6
Undecanoic acid, 10-methyl-, methyl ester	554144	–5	–6.5	–5	–6.4	–4.9
.beta.-D-Glucopyranoside, methyl	2108	–7.3	–6	–5.4	–6	–5.7
12-Bromododecanoic acid	175468	–5.2	–6.1	–5.5	–6.1	–6.1
n-Hexadecanoic acid	985	–5.4	–6.8	–5.3	–6.5	–6.9
Tetradecanoic acid	11005	–5.7	–6.2	–5.2	–6.3	–6.5
Oleic Acid	445639	–6	–6.4	–5.7	–6.6	–5.6
2-Methyl-Z,Z-3,13-octadecadienol	5364412	–5.8	–7.1	–5.7	–6.4	–7.3
2-octyl-Cyclopropaneoctanal	550143	–5.9	–6.8	–5.4	–6.4	–4.5
Z-(13,14-Epoxy)tetradec-11-en-1-ol acetate	5363633	–5.3	–6.4	–5.2	–6.6	–6.8
Oxirane, tridecyl-	86768	–5.1	–6.7	–5.2	–6.2	–5.8
cis-7,cis-11-Hexadecadien-1-yl acetate	5363265	–5.6	–7.4	–5.8	–6.5	–5.5
(Z)-13-Octadecenal	5364497	–5.3	–6.6	–5.3	–6.3	–7.2
*Pyrimethamine	4993	–6.8	–7.0	–6.9	–7.0	–6.0
*Hydroxychloroquine	3652	–7.1	–7.5	–7.1	–7.6	–7.5

Note: *Standard drugs (control) are asterisked.

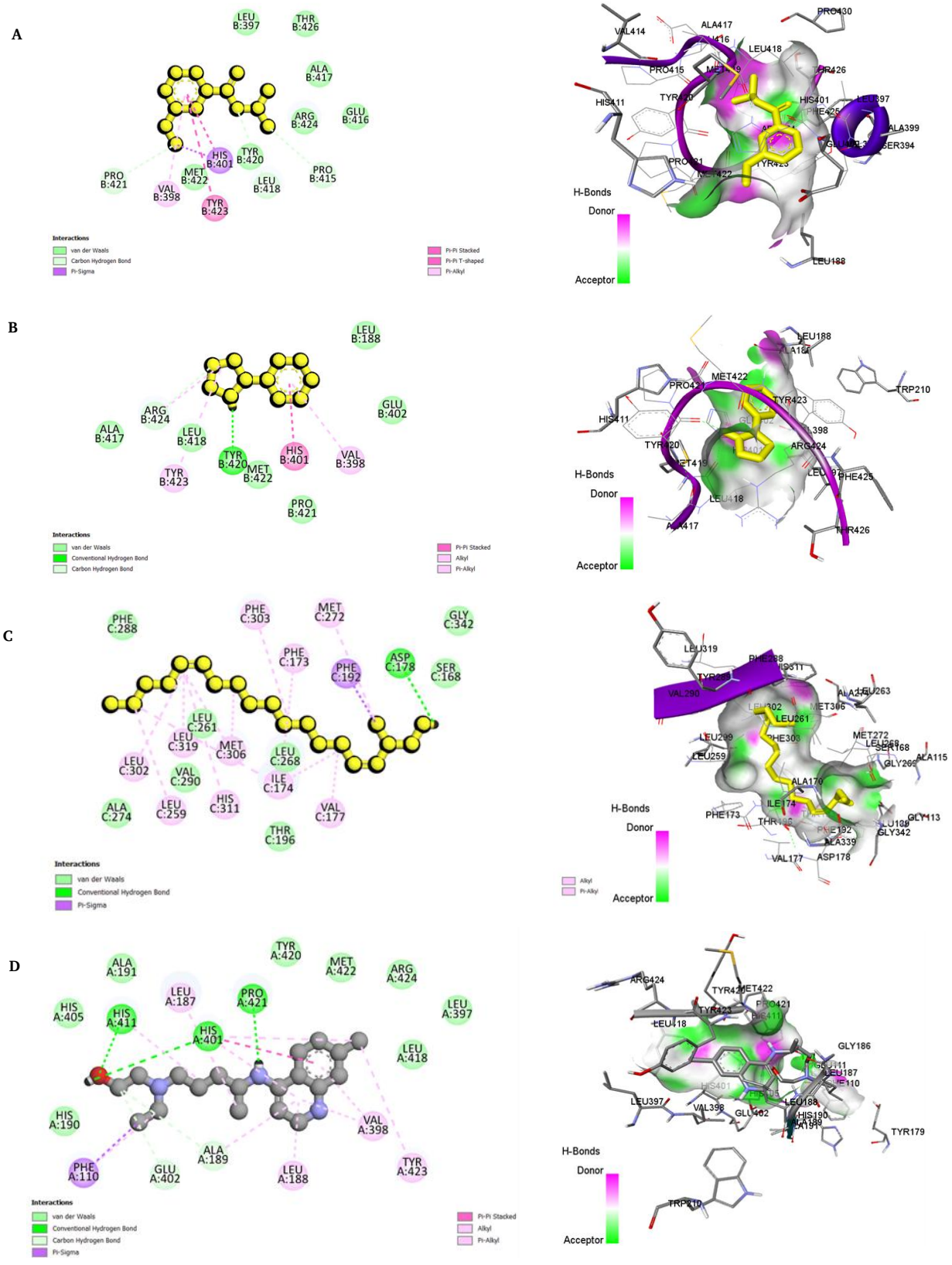

Figure 7 (A-D) Molecular Interactions of amino acid residues in 2D (Left) and 3D (Right) visuals of (A) MMP9-2-Dimethylamino-3'-methoxyacetophenone complex (B) MMP9-3-Phenyl-2-Isoxazoline complex (C) SPHK1-2-Methyl-Z,Z-3,13-octadecadienol complex (D) MMP9-Hydroxychloroquine complex.

The outcome of Molecular Dynamics Simulation

In this study, three parameters of molecular dynamics simulation, including Root Mean Square Deviation (RMSD), Root Mean Square Fluctuation (RMSF), and Radius of gyration (Rg), were considered in assessing the stability, flexibility, and compactness of the best complexes from the Leave extract of *Lawsonia inermis*. Figure 8 shows the average RMSD of (a) MMP9-2-Dimethylamino-3'-methoxyacetophenone complex to be around 2.5 Å at 25 ns and keeping stability till 100 ns (b) MMP9-3-phenyl-2-Isoxazolin to be around 2.4 Å, and staying relatively stable across the 100 ns time frame. Meanwhile, Figure 9 shows the average RMSD of (a) SPHK1-2-Methyl-Z, Z-3,13-octadecadienol to be fairly stable at around 1.6 Å while the (b) standard drug-protein complex expressed more displacement at 3.0 Å, albeit being relatively stable across the 100 ns. Figure 10–11 showed that all the proteins expressed fluctuations with MMP9-2-Dimethylamino-3'-methoxyacetophenone and MMP9-3-phenyl-2-Isoxazoline showing significant changes at residue index of between 60 and 80 and at least 4.0 Å as the peak. Contrarily, SPHK1-2-Methyl-Z, Z-3,13-octadecadienol, and MMP9-Hydroxychloroquine expressed more significant fluctuations with at least 4.5 Å and 6.0 Å, respectively. Figure 12 (A-D) shows the Rg plots with an average value of 3.15 Å, 2.52 Å, 5.4 Å, and 4.5 Å for MMP9-2-Dimethylamino-3'-methoxyacetophenone, MMP9-3-phenyl-2-Isoxazoline, SPHK1-2-Methyl-Z, Z-3,13-octadecadienol and MMP9-Hydroxychloroquine, respectively. Apparently, the first two complexes have better compactness compared to SPHK1-2-Methyl-Z, Z-3,13-octadecadienol, and MMP9-Hydroxychloroquine across 100 ns of simulated physiological conditions. Hence, it is worth noting that MMP9-2-Dimethylamino-3'-methoxyacetophenone and MMP9-3-phenyl-2-Isoxazoline are reliably more stable and compact as receptor-ligand complex for the treatment of *P. falciparum* Malaria compared to 2-Methyl-Z, Z-3,13-octadecadienol and the standard drug, Hydroxychloroquine.

Discussion

Despite the several efforts put into the control and elimination of Malaria prevalence in Africa, thousands of deaths due to Malaria disease are still being reported. This is largely because of the growing resistance of the pathogen, especially *P. falciparum*, against the currently available drugs, including hydroxychloroquine, pyrimethamine, and quinine [31]. Fortunately, several researchers in Nigeria and across Africa are working to find potent phytocompounds with antimalarial properties in herbal plants [32, 33]. In this regard, *Lawsonia inermis* is a widely reported herbal plant that is locally used for Malaria disease treatment in Nigeria. Several *in vitro* and *in vivo* works have documented the antimalarial activities of *Lawsonia inermis* against strains of the Plasmodium pathogen [34, 35]. However, there is a paucity of studies on the mechanism of antiplasmodial activity of the herbal plant against Malaria disease. Understanding the mechanism of action creates an opportunity to find potential targets and drug leads that can be further developed into an effective drug against the notorious disease.

From *Lawsonia inermis* Leaves, fifty-eight phytocompounds were identified, with a good number of alkanes, esters, ketones, alkanol, esters, aromatics, ethers, alkenes, lactones, nitro compounds, and ethers functional groups present. The findings are like those reported by [36]. However, the higher number reported in this study could have been due to the use of solvents with a wide polarity range (Dichloromethane and Methanol). The presence of multiple phytocompounds in *Lawsonia inermis* has been attributed to various therapeutic activities, including the treatment of microbial infection and parasitic infection [13]. Adsorption, Digestion, Metabolism, Excretion, and Toxicity (ADMET) and druglikeness screenings were handy in predicting phytocompounds that are most likely to have the

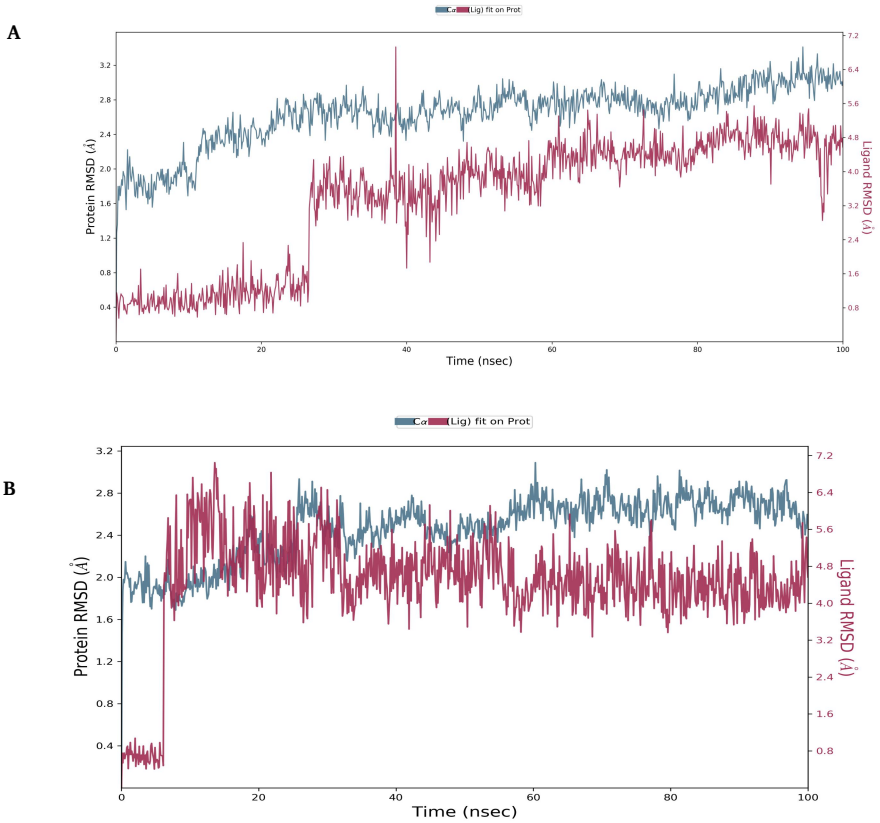

Figure 8 RMSD plots represents the stability between the heavy backbone atoms of proteins and ligand of: (A) MMP9-2-Dimethylamino-3'-methoxyacetophenone and (B) MMP9-3-phenyl-2-Isoxazoline.

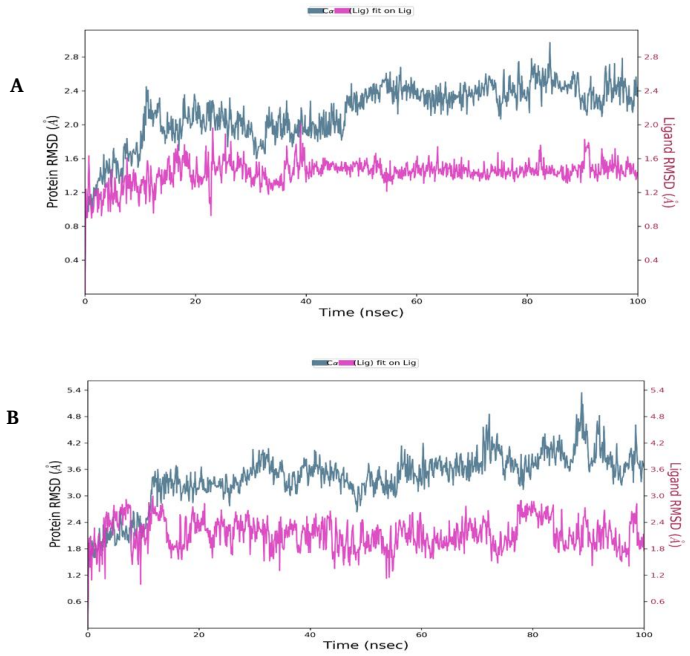

Figure 9 RMSD plots represents the stability between the heavy backbone atoms of proteins and ligand of: (A) SPHK1-2-Methyl-Z,Z-3,13-octadecadienol and (B) MMP9-Hydroxychloroquine.

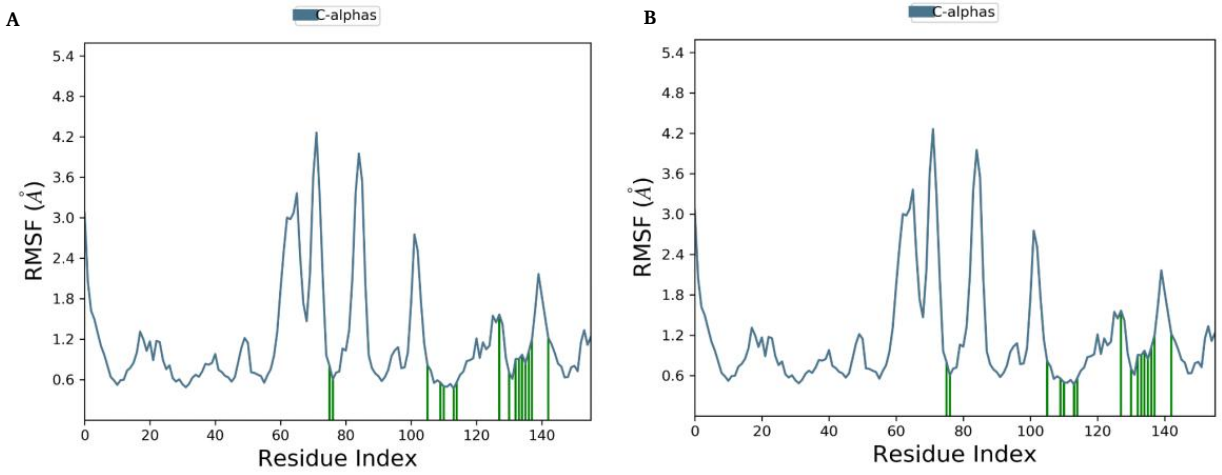

Figure 10 RMSF plot indicating the fluctuation of the proteins during simulation for (A) MMP9-2-Dimethylamino-3'-methoxyacetophenone and (B) MMP9-3-phenyl-2-Isoxazoline.

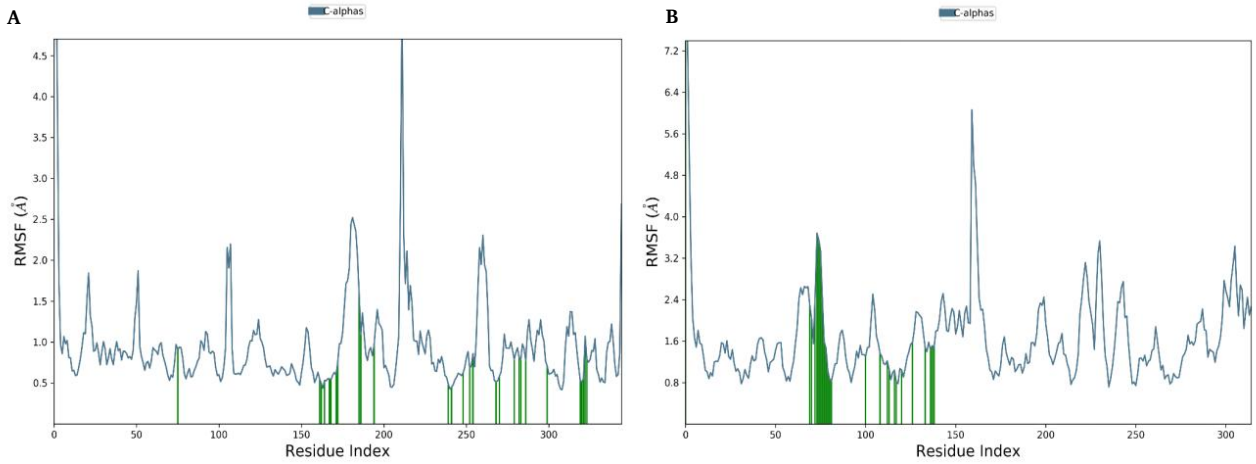

Figure 11 RMSF plot indicating the fluctuation of the proteins during simulation for (A) SPHK1-2-Methyl-Z,Z-3,13-octadecadienol and (B) MMP9-Hydroxychloroquine.

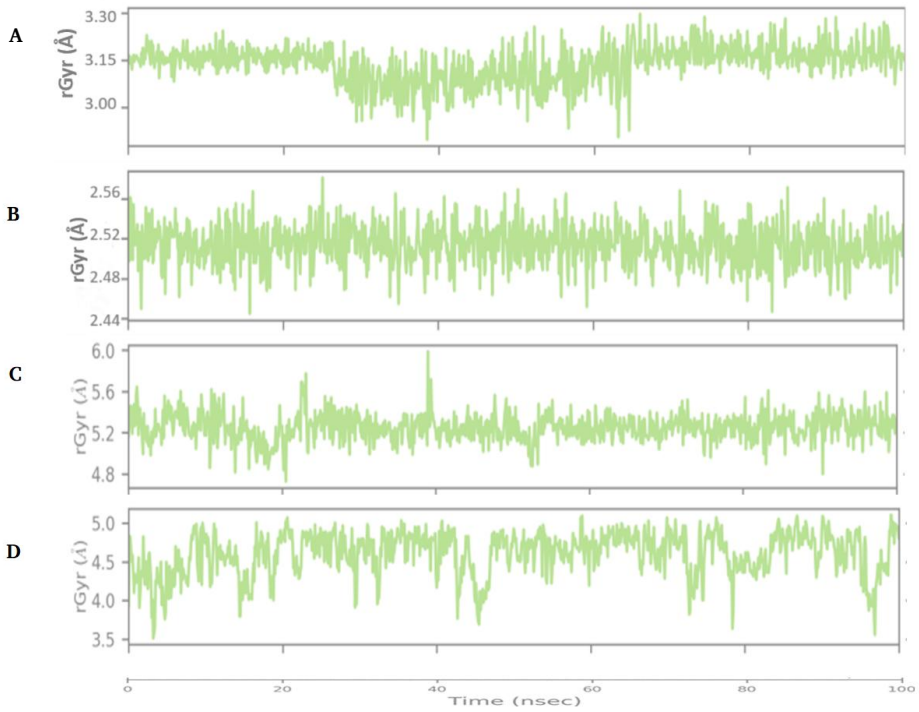

Figure 12 The radius of gyration plot for protein and ligand complexes, including (A) MMP9-2-Dimethylamino-3'-methoxyacetophenone (546935), (B) MMP9-3-phenyl-2-Isoxazoline (840162) (C) SPHK1-2-Methyl-Z,Z-3,13-octadecadienol and (D) MMP9-Hydroxychloroquine. The smaller Rg values indicate tight packing of the ligand throughout the simulation period while a higher value indicates floppy packing.

desired effect when treating Malaria by traditional practitioners. Only twelve phytocompounds were predicted to have favorable ADMET properties and are likely to emerge as lead compounds without health safety concerns. Among the phytocompounds include Boronic acid, ethyl-, bis (2-mercaptoethyl ester); 2-Methyl-1-diisopropylsilyloxypropane; Propionic acid, 2-mercapto-, allyl ester; 3-phenyl-2-Isoxazoline; 2H-Pyran-3-ol, tetrahydro-6-methoxy-2-methyl-, [2R-(2.alpha., 3.beta., 6.beta.)] and 2-[2-(2-mercaptoethoxy)ethoxy]-Ethanol. Many of these phytocompounds have been reported as bioactives. In 2022, boronic acids were reported for biological activities, including antibacterial, anticancer, and antiviral actions [37]. Also, the derivatives of isoxazoline, including 3-phenyl-2-Isoxazoline, have been observed to have pharmacological and biological activities, including anti-inflammatory, antifungal, anticancer, and antimicrobial actions [38]. This is largely due to the interactions of most phytocompounds with plasma protein and cytochrome enzymes and their ability to serve as a substrate to P-glycoproteins. Such interactions have been reported to result in unwanted adverse effects and potentially toxic due to lower clearance and accumulation of drugs and/or their metabolites [39]. However, the majority of the phytocompounds passed Lipinski's rules for the drug-likeness test, with only Paromomycin violating more than one rule. This is probably because Lipinski's rule focuses only on the physicochemical properties of the compounds, including the number of hydrogen bond acceptors, the number of hydrogen bond donors, lipophilicity, and molecular weight [40].

To understand the relationship among the genes that selected phytocompounds from *Lawsonia inermis* Leaves extract can interact with, a protein-protein network was developed to show the relationship among the proteins. Proteins with more lines (edges) interact more and are likely to modulate the activity of other proteins. The maximal clique centrality (MCC) analysis revealed that Proto-oncogene tyrosine-protein kinase (SRC), Heat shock protein 90-alpha (HSP90AA1), and Vascular endothelial growth factor A (VEGFA) are the top three most essential proteins in the interactions. Protein kinases have been reported to participate in parasite growth, maturation, and differentiation functions across the lifecycle stages of *P. falciparum* [41]. Canavese and Spaccapelo note an overexpression of VEFGA in the brain tissue of patients with cerebral Malaria [42]. The HSP90AA1 are proteins in both the *Plasmodium falciparum* and humans. The PfHSP90 is necessary for parasite development as it is involved in its development regulation during frequent febrile episodes [43]. However, targeting the protein is not an option, as knocking down the homolog in humans can increase the chances of abdominal pain [44].

To further understand the mechanism of bioactive action in LIL, KEGG pathways and gene ontology analysis were carried out. The gene function analysis of LIL phytocompounds shows the most significant enrichment in inflammatory response, with the highest percentage of the genes present in the plasma membrane, cytoplasm, and cytosol. Most of the genes play active roles in adenosine triphosphate binding, enzyme binding, and heme binding. Hemozoin pigment and lipid-associated anchors are known to be released during the breaking down of the infected erythrocytes, leading to a response from the immune system [45]. The innate immune system responds via innate receptor signaling. This results in the inducement of pro-inflammatory mediators such as TNF-alpha, NOS2, IL-8 IFN-gamma, IL-1, and IL-6 [46]. These mediators play crucial roles in controlling the growth of the Plasmodium parasite and its elimination, as a balance must exist between the pro-inflammatory and anti-inflammatory responses. This is maintained by IL-10 and the transforming growth factor (TGF) [47]. With phytocompounds from *Lawsonia inermis* Leaves focusing on genes involved in an inflammatory response, it is possible that the herbal plant mechanism of action centers on their interactions with MMP9, MAPK1, HMOX1, IDO1, TLR4, VCAM1, and other proteins involved in metabolism and signaling pathways. This is in line with the report of [16], as the *in vivo* study showed that *Lawsonia inermis* extract suppressed parasitemia through inflammatory cytokine modulation, notably IL-6, TNF-alpha, and IL-10.

This is also supported by the result from KEGG pathway analysis with metabolic pathways, PI3K-Akt signaling pathway, and HIF-1 signaling pathway having genes involved in inflammation. The

Maximal Clique Centrality analysis of the network pharmacology predicted that the twelve phytocompounds could modulate sixty-nine proteins involved in forty-one signaling pathways. This suggests that multiple compounds from LIL can interact with multiple proteins involved in various diseases. Several of the phytoconstituents are hit compounds for multiple targets, such as 2-[2-(2-mercaptoethoxy) ethoxy]-Ethanol that interacts with thirty proteins; Boronic acid ethyl-bis(2-mercaptoethyl ester interacts with nineteen proteins while Chlorocarbonylsulfenyl chloride interacts with twenty-two proteins. Mitogen-activated protein Kinase 1 (MAPK1), Proto-oncogene tyrosine-protein kinase (SRC), and Platelet-derived growth factor receptor β (PDGFRβ) are the top three most modulated proteins in the network. Some of these proteins have been reported to be potential drug targets for Malaria and other diseases. For instance, Sphingosine kinase 1 (SPHK1) has been reported to be a potent antimalarial drug target as its inhibition halt parasite growth in *P. falciparum* infection [48]; inhibitors of MAPK1 have been reported to obstruct the replication of *P. falciparum* in human erythrocytes [49]; Protein Kinase CAMP-Activated Catalytic Subunit Alpha (PRKACA) as a novel target for hepatocellular carcinoma [50]; inhibition of MMP9 in ischemic stroke treatment [51]; and Cyclin-dependent kinase-5 (CDK5) as a drug target for Alzheimer's disease [52]. The synergistic interactions of LIL phytocompounds consolidate the multi-therapeutic values of the herbal plant, including *P. falciparum* Malaria, as previously reported by different studies [13, 14].

Additionally, the molecular docking approach was used to validate and view the interaction of the phytocompounds in *Lawsonia inermis* against some of the core proteins from network pharmacology that have been reported to be potential drug targets for treating *P. falciparum* Malaria. The selected targets include Glycogen synthase kinase-3 beta (GSK3β), Mitogen-Activated Protein Kinase 1 (MAPK1), Sphingosine kinase 1 (SPHK1), Indoleamine 2,3dioxygenase 1 (IDO1) and Matrix metalloproteinase-9 (MMP9). In addition to the binding affinity score of the complex and ADMET profile of the ligand, the type of interaction and presence of unfavorable bonds were considered in choosing complexes for further analysis. Consequently, MMP9-3-phenyl-2-Isoxazoline (840162), SPHK1-2-Methyl-Z, Z-3,13-octadecadienol (5364412) and MMP9-2-Dimethylamino-3'-methoxyacetophenone (546935) form the most favorable complexes for *antimalaria* treatment by phytocompounds from *Lawsonia inermis* herbal plant.

Using the molecular dynamics simulation approach, the stability and flexibility of the complexes, including the best complex by standard drug, in the simulated physiological environment were assessed. The RMSD value that measures the stability of the complex across 100ns shows that 2-Dimethylamino-3'-methoxyacetophenone and 3-phenyl-2-Isoxazoline form reliably more stable complexes with the targets compared to 2-Methyl-Z, Z-3,13-octadecadienol, and Hydroxychloroquine. However, it is also worth mentioning that 2-Methyl-Z, Z-3,13-octadecadienol from the leaf extract of *Lawsonia inermis* had a great interaction with SPHK1. By assessing the compactness and stability of the phytocompound against the target over a 100ns period, it is apparent that the efficacy of the potential drug candidate could be compromised due to significant fluctuation in the binding pocket of the protein. This could be due to more hydrogen bond and hydrophobic bond interactions between the 2-Dimethylamino-3'-methoxyacetophenone and 3-phenyl-2-Isoxazoline phytocompounds and MMP9 compared to the standard drug and 2-methyl-z, Z-3,13-octadecadienol. According to Kurzab et al., hydrogen bonds serve as the most crucial force in stabilizing biological systems. This is because they are essential for recognizing ligand-reception, stabilizing the tertiary structure of the target, and enabling the movement of protons in enzymatic reactions [53]. Nevertheless, salt bridge and hydrophobic interactions must be considered in assessing a ligand-target system as they contribute significantly to optimizing drugs for improved efficacy [54]. The 2-Dimethylamino-3'methoxyacetophenone interacted with PRO415, PRO421 and LEU418 using carbon-hydrogen bonds, alongside the heavy presence of hydrophobic bonds, including Pi-Pi Stacked, Pi-Pi T-Shaped, Pi-Alkyl, and Pi-Sigma, with TYR423, VAL398 and HIS401 amino acid residues of MMP9 protein. As for 3-phenyl-2-Isoxazoline from *Lawsonia inermis* plant, it formed a conventional hydrogen bond with TYR420 and a carbon-hydrogen bond with ARG424, alongside a Pi-Pi Stacked bond, Alkyl bond, and Pi-Alkyl bond interaction with HIS401, VAL398, and TYR423 of MMP9 protein, respectively. The heavy presence of these hydrogen bonds and hydrophobic interactions compared to the lesser presence in SPHK1-2-Methyl-Z, Z-3,13-octadecadienol could be responsible for their better stability and compactness. In other words, the significant presence of hydrogen bonds and hydrophobic interactions between the protein-ligand complexes encourages flexibility, which is further validated by displacement of the protein (RMSF) and compactness of the complex (radius of gyration) results. This informs that complexes cannot be solely judged based on binding affinity score. Instead, the interactions and performance of complexes within a physiological environment should be highly considered. Besides, the two compounds, especially 3-phenyl-2-Isoxazoline, have better adsorption, distribution, metabolism, excretion, and toxicity profiles compared to the standard drug. This aligns with the findings of Omoboyowa and colleagues, who note that protein-ligand complexes with hydrogen bonds and hydrophobic interactions are more likely to express good ADMET profiles regarding adsorption, metabolism, and distribution [55]. With the average cost of Malaria prevention and treatment ranging from 5 to 50 USD in Africa [56], the better ADMET profiles of these drug candidates are likely to encourage a more affordable and cost-effective solution.

Conclusion

Based on GC-MS analysis of *Lawsonia inermis* leaf extract, the plant contains an abundance of phytocompounds with pharmacological values. By using a network pharmacology approach, the antimalarial activity of *Lawsonia inermis* works by the interaction of phytocompounds in the plants with genes involved in inflammatory responses via their binding with core proteins in metabolic and signaling pathways. Based on the outcome of the computational studies, it is evident that 3-phenyl-2-Isoxazoline and 2-Dimethylamino-3'-methoxyacetophenone from the leaves of *Lawsonia inermis* are potent inhibitors of MMP9, a potential drug target of *P. falciparum* Malaria. Overall, the application of network pharmacology, molecular docking and molecular dynamics simulation shows that *Lawsonia inermis* does not only have therapeutic values but contains multiple phytocompounds with the ability to modulate multiple proteins and pathways in the treatment of various diseases, including notorious Malaria. Thus, it is recommended that wet-lab studies should be carried out on the antimalarial activity of 3-phenyl-2-Isoxazoline and 2-Dimethylamino-3'-methoxyacetophenone from *Lawsonia inermis* plant against Matrix metalloproteinase-9 (MMP9) for further assessment and towards drug discovery.

References

1. Nkumama IN, O'Meara WP, Osier FHA. Changes in Malaria Epidemiology in Africa and New Challenges for Elimination. *Trends Parasitol.* 2017;33(2):128–140. Available at: http://doi.org/10.1016/j.pt.2016.11.006
2. Ashley EA, Phyo AP. Drugs in Development for Malaria. *Drugs.* 2018;78(9):861–879. Available at: http://doi.org/10.1007/s40265-018-0911-9
3. Venugopal K, Hentzschel F, Valkiūnas G, Marti M. Plasmodium asexual growth and sexual development in the haematopoietic niche of the host. *Nat Rev Microbiol.* 2020;18(3):177–189. Available at: http://doi.org/10.1038/s41579-019-0306-2
4. World Health Organization; 2023. Fact sheet about Malaria. https://www.who.int/news-room/fact-sheets/detail/Malaria#:~:text=According%20to%20the%20latest%20World.

5. World Health Organization; 2021. WHO recommends groundbreaking Malaria vaccine for children at risk. https://www.who.int/news/item/06-10-2021-who-recommends-groundbreaking-Malaria-vaccine-for-children-at-risk Accessed 23 October 2022.
6. Turkson B K, Agyemang A O, Nkrumah D, et al. Treatment of malaria infection and drug resistance. *Plasmodium Species and Drug Resistance*. IntechOpen, 2021.
7. Mishra M, Mishra VK, Kashaw V, Iyer AK, Kashaw SK. Comprehensive review on various strategies for antimalarial drug discovery. *Eur J Med Chem.* 2017;125:1300–1320. Available at: http://doi.org/10.1016/j.ejmech.2016.11.025
8. Shibeshi M A, Kifle Z D, Atnafie S A. Antimalarial drug resistance and novel targets for antimalarial drug discovery. Infect and Drug Resist. 2020;13:4047–4060. Available at: https://doi.org/10.2147/IDR.S279433
9. Mishra M, Mishra VK, Kashaw V, Iyer AK, Kashaw SK. Comprehensive review on various strategies for antimalarial drug discovery. *Eur J Med Chem.* 2017;125:1300–1320. Available at: http://doi.org/10.1016/j.ejmech.2016.11.025
10. Verma AK, Kumar M, Bussmann RW. Medicinal plants in an urban environment: the medicinal flora of Banares Hindu University, Varanasi, Uttar Pradesh. *J Ethnobiol Ethnomed.* 2007;3:35. Available at: http://doi.org/10.1186/1746-4269-3-35
11. Kamaraj C, Ragavendran C, Prem P, et al. Exploring the Therapeutic Potential of Traditional Antimalarial and Antidengue Plants: A Mechanistic Perspective. *Can J Infect Dis Med Microbiol*. 2023;2023:1860084. Available at: http://doi.org/10.1155/2023/1860084
12. Afolayan FID, Adegbolagun OM, Irungu B, Kangethe L, Orwa J, Anumudu CI. Antimalarial actions of Lawsonia inermis, Tithonia diversifolia and Chromolaena odorata in combination. *J Ethnopharmacol.* 2016;191:188–194. Available at: http://doi.org/10.1016/j.jep.2016.06.045
13. AL-SNAFI AE. A review on Lawsonia inermis: A potential medicinal plant. *Int J Curr Pharm Sci September.* 2019;11(5):1–13. Available at: http://doi.org/10.22159/ijcpr.2019v11i5.35695
14. Afolayan FID, Adegbolagun OM, Irungu B, Kangethe L, Orwa J, Anumudu CI. Antimalarial actions of Lawsonia inermis, Tithonia diversifolia and Chromolaena odorata in combination. *J Ethnopharmacol.* 2016;191:188–94. Available at: http://doi.org/10.1016/j.jep.2016.06.045
15. El Babili F. Lawsonia Inermis: Its Anatomy and its Antimalarial, Antioxidant and Human Breast Cancer Cells MCF7 Activities. *Pharmt Anal Acta.* 2013;4(1):2–6. Available at: http://doi.org/10.4172/2153-2435.1000203
16. Afolayan FID, Adegbolagun O, Mwikwabe NN, Orwa J, Anumudu C. Cytokine modulation during malaria infections by some medicinal plants. *Sci Afr.* 2020;8:e00428. Available at: http://doi.org/10.1016/j.sciaf.2020.e00428
17. Batiha GE-S, Teibo JO, Shaheen HM, et al. Therapeutic potential of Lawsonia inermis Linn: a comprehensive overview. *Naunyn Schmiedebergs Arch Pharmacol.* 2023. Available at: http://doi.org/10.1007/s00210-023-02735-8
18. Yuan J, Zhu Y, Zhao J, et al. Network Pharmacology, Molecular Docking and Molecular Dynamics Simulation Studies of the Molecular Targets and Mechanisms of ChuanKeZhi in the Treatment of COVID-19. *Nat Prod Commun.* 2022;17(8):1934578X2211169. Available at: http://doi.org/10.1177/1934578X221116977
19. Wu Y, Zhu Y, Xie N, et al. A network pharmacology approach to explore active compounds and pharmacological mechanisms of a patented Chinese herbal medicine in the treatment of endometriosis. *PLoS One.* 2022;17(2):e0263614. Available at: https://doi.org/10.1371/journal.pone.0263614
20. Ferreira LLG, Andricopulo AD. ADMET modeling approaches in drug discovery. *Drug Discov Today.* 2019;24(5):1157–1165. Available at: http://doi.org/10.1016/j.drudis.2019.03.015
21. Afolayan FID, Ijidakinro OD. In silico antiparasitic investigation of compounds derived from Andrographis paniculata on some parasites validated drug targets. *Afr J Biol Sci.* 2021;3(3):93–110. Available at: http://doi.org/10.33472/AFJBS.3.3.2021.93-110
22. Xiong G, Wu Z, Yi J, et al. ADMETlab 2.0: an integrated online platform for accurate and comprehensive predictions of ADMET properties. *Nucleic Acids Res.* 2021;49(W1):W5–W14. Available at: https://doi.org/10.1093/nar/gkab255
23. Banerjee P, Eckert AO, Schrey AK, Preissner R. ProTox-II: a webserver for the prediction of toxicity of chemicals. *Nucleic Acids Res.* 2018;46(W1):W257–W63. Available at: http://doi.org/10.1093/nar/gky318
24. Liang B, Li C, Zhao J. Identification of key pathways and genes in colorectal cancer using bioinformatics analysis. *Med Oncol.* 2016;33(10):111. Available at: http://doi.org/10.1007/s12032-016-0829-6
25. Huang X-F, Zhang J-L, Huang D-P, et al. A network pharmacology strategy to investigate the anti-inflammatory mechanism of luteolin combined with in vitro transcriptomics and proteomics. *Int Immunopharmacol.* 2020;86:106727. Available at: http://doi.org/10.1016/j.intimp.2020.106727
26. Li LZ, Wang HY, Huang JH, et al. The Mechanism of Dendrobium officinale as a Treatment for Hyperlipidemia Based on Network Pharmacology and Experimental Validation. *Evid Based Complement Alternat Med.* 2022;2022:5821829. Available at: https://doi.org/10.1155/2022/5821829
27. Johnson TO, Odoh KD, Nwonuma CO, Akinsanmi AO, Adegboyega AE. Biochemical evaluation and molecular docking assessment of the anti-inflammatory potential of Phyllanthus nivosus leaf against ulcerative colitis. *Heliyon.* 2020;6(5):e03893. Available at: http://doi.org/10.1016/j.heliyon.2020.e03893
28. Hildebrand PW, Rose AS, Tiemann JKS. Bringing Molecular Dynamics Simulation Data into View. *Trends Biochem Sci.* 2019;44(11):902–913. Available at: http://doi.org/10.1016/j.tibs.2019.06.004
29. Rasheed MA, Iqbal MN, Saddick S, et al. Identification of Lead Compounds against Scm (fms10) in Enterococcus faecium Using Computer Aided Drug Designing. *Life.* 2021;11(2):77. Available at: http://doi.org/10.3390/life11020077
30. Shivakumar D, Williams J, Wu Y, Damm W, Shelley J, Sherman W. Prediction of Absolute Solvation Free Energies using Molecular Dynamics Free Energy Perturbation and the OPLS Force Field. *J Chem Theory Comput.* 2010;6(5):1509–1519. Available at: http://doi.org/10.1021/ct900587b
31. Kozlov M. Resistance to front-line malaria drugs confirmed in Africa. *Nature.* 2021;597(7878):604. Available at: http://doi.org/10.1038/d41586-021-02592-6
32. Ibrahim ZY, Uzairu A, Shallangwa GA, Abechi SE. Molecular modeling and design of some β-amino alcohol grafted 1,4,5-trisubstituted 1,2,3-triazoles derivatives against chloroquine sensitive, 3D7 strain of Plasmodium falciparum. *Heliyon.* 2021;7(1):e05924. Available at: http://doi.org/10.1016/j.heliyon.2021.e05924
33. Afolayan FID, Ibrahim S. Computational simulations of phytoconstituents derived from Phyllanthus amarus against Plasmodium falciparum molecular targets. *Drug Discovery.* 2023;17:e26dd1937.
34. Afolayan F, Anumudu CI, Adegbolagun OM, et al. In vitro

antiplasmodial activity and cytotoxicity of some medicinal plants indigenously used in Nigeria against Malaria. Proceedings of the 4th Walter Sisulu University International Research Conference; 2014.
35. Alaribe CS, Oladipupo AR, Nani MO, Ijeoma IN, Olanipekun BD, Coker HAB. Suppressive and curative antiplasmodial properties of Nauclea latifolia root extract and fractions against erythrocytic stage of mice-infective chloroquine-sensitive Plasmodium berghei NK-65. *J Med Plants Econ Dev.* 2020;4(1):1–6. Available at: http://doi.org/10.4102/jomped.v4i1.72
36. Hassan WN. Phytochemical Analysis of Nigerian and Egyptian Henna (Lawsonia Inermis L.) Leaves using TLC, FTIR and GCMS. *Plant*. 2014;2(3):27–32. Available at: https://doi.org/10.11648/j.plant.20140203.11
37. Silva MP, Saraiva L, Pinto M, Sousa ME. Boronic Acids and Their Derivatives in Medicinal Chemistry: Synthesis and Biological Applications. *Molecules.* 2020;25(18):4323. Available at: http://doi.org/10.3390/molecules25184323
38. El Idrissi M, El Ghozlani M, Eşme A, et al. Mpro-SARS-CoV-2 Inhibitors and Various Chemical Reactivity of 1-Bromo- and 1-Chloro-4-vinylbenzene in [3 + 2] Cycloaddition Reactions. *Organics.* 2021;2(1):1–16. Available at: http://doi.org/10.3390/org2010001
39. Daina A, Michielin O, Zoete V. SwissADME: a free web tool to evaluate pharmacokinetics, drug-likeness and medicinal chemistry friendliness of small molecules. *Sci Rep.* 2017;7:42717. Available at: http://doi.org/10.1038/srep42717
40. Lipinski CA. Lead- and drug-like compounds: the rule-of-five revolution. *Drug Discov Today Technol.* 2004;1(4):337–341. Available at: http://doi.org/10.1016/j.ddtec.2004.11.007
41. Sharma A. Protein tyrosine kinase activity in human Malaria parasite Plasmodium falciparum. *Indian J Exp Biol.* 2000;38(12):1222–1226. Available at: https://pubmed.ncbi.nlm.nih.gov/11411043/
42. Canavese M, Spaccapelo R. Protective or pathogenic effects of vascular endothelial growth factor (VEGF) as potential biomarker in cerebral malaria. *Pathog Global Health.* 2014;108(2):67–75. Available at: http://doi.org/10.1179/2047773214Y.0000000130
43. Ramdhave A, Patel D, Ramya I, Nandave M, Kharkar P. Targeting Heat Shock Protein 90 for Malaria. *Mini Rev Med Chem.* 2013;13(13):1903–1920. Available at: http://doi.org/10.2174/13895575113136660094
44. Miles VN, Patel RK, Smith AG, McCall RP, Wu J, Lei W. The Effect of Heat Shock Protein 90 Inhibitor on Pain in Cancer Patients: A Systematic Review and Meta-Analysis. *Medicina (Kaunas).* 2020;57(1):5. Available at: http://doi.org/10.3390/medicina57010005
45. Penha-Gonçalves C. Genetics of Malaria Inflammatory Responses: A Pathogenesis Perspective. *Front Immunol.* 2019;10:1771. Available at: http://doi.org/10.3389/fimmu.2019.01771
46. Gowda DC. TLR-mediated cell signaling by malaria GPIs. *Trends Parasitol.* 2007;23(12):596–604. Available at: http://doi.org/10.1016/j.pt.2007.09.003
47. Popa GL. Popa MI. Recent Advances in Understanding the Inflammatory Response in Malaria: A Review of the Dual Role of Cytokines. J Immunol Res. 2021;2021:7785180. Available at: https://doi.org/10.1155/2021/7785180
48. Sah RK, Pati S, Saini M, et al. Reduction of Sphingosine Kinase 1 Phosphorylation and Activity in Plasmodium-Infected Erythrocytes. *Front Cell Dev Biol.* 2020;8:80. Available at: http://doi.org/10.3389/fcell.2020.00080
49. Brumlik MJ, Nkhoma S, Kious MJ, et al. Human p38 mitogen-activated protein kinase inhibitor drugs inhibit Plasmodium falciparum replication. *Exp Parasitol.* 2011;128(2):170–175. Available at: http://doi.org/10.1016/j.exppara.2011.02.016
50. Toyota A, Goto M, Miyamoto M, et al. Novel protein kinase cAMP-Activated Catalytic Subunit Alpha (PRKACA) inhibitor shows anti-tumor activity in a fibrolamellar hepatocellular carcinoma model. *Biochem Biophys Res Commun.* 2022;621:157–161. Available at: http://doi.org/10.1016/j.bbrc.2022.07.008
51. Luo S, Li H, Mo Z, et al. Connectivity map identifies luteolin as a treatment option of ischemic stroke by inhibiting MMP9 and activation of the PI3K/Akt signaling pathway. *Exp Mol Med.* 2019;51(3):1–11. Available at: http://doi.org/10.1038/s12276-019-0229-z
52. Lau L-F, Seymour PA, Sanner MA, Schachter JB. Cdk5 as a Drug Target for the Treatment of Alzheimer's Disease. *J Mol Neurosci.* 2002;19(3):267–273. Available at: http://doi.org/10.1385/JMN:19:3:267
53. Kurczab R, Śliwa P, Rataj K, Kafel R, Bojarski AJ. Salt Bridge in Ligand–Protein Complexes—Systematic Theoretical and Statistical Investigations. *J Chem Inf Model.* 2018;58(11):2224–2238. Available at: http://doi.org/10.1021/acs.jcim.8b00266
54. Patil R, Das S, Stanley A, et al. Optimized Hydrophobic Interactions and Hydrogen Bonding at the Target-Ligand Interface Leads the Pathways of Drug-Designing. *PLoS One.* 2010;5(8):e12029. Available at: https://doi.org/10.1371/journal.pone.0012029
55. Omoboyowa DA, Balogun TA, Omomule OM, Saibu OA. Identification of Terpenoids FromAbrus precatoriusAgainst Parkinson's Disease Proteins UsingIn SilicoApproach. *Bioinform Biol Insights.* 2021;15:117793222110507. Available at: http://doi.org/10.1177/11779322211050757
56. Cirera L, Sacoor C, Meremikwu M, et al. The economic costs of Malaria in pregnancy: evidence from four sub-Saharan countries. *Gates Open Res*. 2023;7:47. Available at: https://doi.org/10.12688/gatesopenres.14375.2